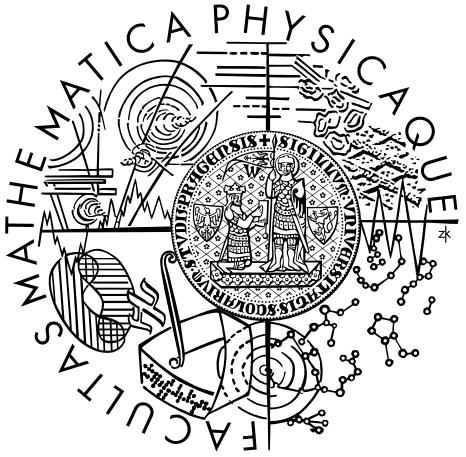

DOCTORAL THESIS

Ján Šubjak

Photometric and spectroscopic characterization of substellar companions to stars

Astronomical Institute of Charles University

Supervisor of the doctoral thesis: Petr Kabáth
Co-supervisor of the doctoral thesis: Nicolas Lodieu

Study programme: Astronomy and Astrophysics

Study branch: Theoretical Physics, Astronomy and Astrophysics

Prague 2022

I declare that I carried out this doctoral thesis independently, and only with the cited sources, literature and other professional sources. It has not been used to obtain another or the same degree.

I understand that my work relates to the rights and obligations under the Act No. 121/2000 Sb., the Copyright Act, as amended, in particular the fact that the Charles University has the right to conclude a license agreement on the use of this work as a school work pursuant to Section 60 subsection 1 of the Copyright Act.

In ..... date ....

Author's signature

I dedicate this thesis to my family, who provided me with their endless support during the years of my PhD studies. To all colleagues and friends I met travelling across Europe who shared their words of wisdom. To my old friends from my little home town who have never stopped bringing joy to my life.

I want to give my special thanks to Dr Petr Kabáth, Dr Nicolas Lodieu and Dr Henri Boffin for their guidance and mentorship in all aspects of my personal and scientific life.

I am also grateful for the financial support from MSMT grant LTT-20015, from ERASMUS+ grant 2020-1-CZ01-KA203-078200, and from the Grant Agency of Charles University: GAUK No. 314421.

Title: Photometric and spectroscopic characterization of substellar companions to stars

Author: Ján Šubjak

Department: Astronomical Institute of Charles University

Supervisor: Petr Kabáth, Astronomical Institute of the Czech Academy of Sciences

Co-supervisor: Nicolas Lodieu, Instituto de Astrofísica de Canarias, Universidad de La Laguna

Abstract: Substellar objects (giants planets and brown dwarfs) are objects not massive enough to sustain hydrogen fusion as stars do. These two groups have many similar properties; hence, the best way to characterise and distinguish them is intensively discussed. One can argue that the current definition based on the mass is not fundamental as it does not include objects in the phase of accreting mass, which can end up either as giant planets or brown dwarfs. Hence, the formation process can be a better approach to distinguishing giant planets from brown dwarfs. However, because of the difficulty in observationally determining the formation history of individual substellar companions to stars, such a definition is very difficult to put into practice. The presented study discusses transiting substellar objects as especially suitable objects to study their formation and evolution history. It presents techniques which can be used to study the formation and evolution of these objects, focusing primarily on the tidal interactions between substellar objects and host stars, and discusses that the precision of stellar parameters such as mass, radius and age play a crucial role. Tidal interactions are then studied for two specific systems of a transiting brown dwarf and Saturn-mass planet. Finally, to understand the formation and evolution of these systems, one must also understand the effect of other bodies. Planetary systems can be significantly affected by wide companions through different processes. The work compares the parameter distributions of known planets around single stars to that with a wide stellar and substellar companion to search for possible peculiarities in their parameter distributions. So far, planets in systems with a wide brown dwarf companion appear to follow their own eccentricity distribution with a maximum at ~ 0.65 and usually have periods larger than 40 days and masses larger than 0.1 mass of Jupiter.

Keywords: spectroscopic techniques: radial velocities, techniques: photometric, planets and satellites: detection, stars: planetary systems, stars: brown dwarfs

Contents

Preface **2**

Aims **5**

1 Introduction **6**
1.1 Brown dwarfs 6
1.2 Giant planets 10
1.3 Stellar parameters 13
1.3.1 Mass and radius 14
1.3.2 Age 16

2 Tidal interactions **26**
2.1 Stellar tidal quality factor 28
2.2 Substellar tidal quality factor 28

3 TOI-503: The first known brown dwarf-Am star binary from the TESS mission **29**

4 TOI-1268b: The youngest hot Saturn-mass transiting exoplanet **30**

5 Search for planets around stars with wide brown dwarfs **31**

Summary and outlook **32**

Bibliography **34**

List of Figures **53**

List of Abbreviations **55**

List of publications **56**

A Šubjak et al. 2020 **77**

B Šubjak et al. 2022a **97**

C Šubjak et al. 2022b **119**

Background

Substellar objects (SSOs) are not massive enough to sustain hydrogen fusion as stars do. In this work, we recognise SSOs as the merged groups of brown dwarfs (BDs) and extrasolar giant planets (EGPs). These two groups have many similar properties (Burrows et al., 2001), such as:

- Their atmospheres are predominantly molecular.
- They have similar radii caused by the electron degeneracy pressure in the interior.
- Thermonuclear processes do not dominate their evolution.
- They cool off in time.
- They share the same trend in the mass-density diagram (Hatzes and Rauer, 2015).

Hence, the best way to characterise and distinguish both groups of objects is intensively debated. One can argue that the definition based only on the mass is not fundamental as it does not include objects in the phase of accreting mass, which can end up either as EGPs or BDs. Burrows et al. (2001) proposed to use the formation process to distinguish giant planets from BDs. As such definition would be defined for objects of all ages, this idea was recognised and further discussed (e.g., Schneider et al., 2011; Wright et al., 2011; Chabrier et al., 2014). In this case, the two processes are formation via core accretion in a protoplanetary disk (the way giant planets are thought to form) and formation by gravitational instability, which is how stars are thought to typically form. However, such a definition would not be consistent with the original one as we would observe an overlap in the mass distributions. Some objects with only a few masses of Jupiter (M_J) that formed like stars by the gravitational collapse of interstellar material would be considered BDs (Padoan and Nordlund, 2004; Hennebelle and Chabrier, 2008). On the other hand, objects with tens M_J that formed via core accretion in protoplanetary discs would be considered planets. Because of the difficulty in observationally determining the formation history of individual substellar companions to stars, such a definition is very difficult to put into practice.

Transiting SSOs are especially suitable for studying their formation and evolution history. They enable us to measure their mass, radius and age, which are key parameters to study the internal composition of these objects and compare it with model predictions. These properties can be linked through the interior structure models to the formation history as SSOs formed by core accretion are believed to contain more heavy elements (Baraffe et al., 2010). Furthermore, many discovered transiting SSOs have orbital periods of the order of days. For such close orbits, tides are strong and significantly affect orbital parameters. SSOs can form via core accretion in the protoplanetary disc behind the snow line at large separations from their host stars and then migrate inwards through interaction with the disc (Coleman et al., 2017). After such migration, the tidal interactions with the host star play a significant role and circularise the orbit on timescales that can

be calculated (Jackson et al., 2008). Comparing the orbital eccentricity, circularisation timescale and age of the system provides implications for how the SSOs may have formed. For example, if we observe SSOs on a close circular orbit and the circularisation timescale is larger than the age of the system, we assume that the object formed in situ at its current distance from the star. To be able to compare the tidal timescales with stellar ages, we assume that migration occurs very early in the lifetime of systems (Trilling et al., 1998; Murray et al., 1998; Suárez Mascareño et al., 2021). The tidal interaction between a close-in companion and its host star also transfers angular momentum from the companion's orbit to the star's rotation and hence changes the properties of the star. For example, these can be linked with the Am phenomenon for A-type stars, as we will discuss later.

Transiting SSOs also provide a unique opportunity to study their atmospheres via transit and eclipse observations. The study of atmospheres can uncover the formation history, which leaves a footprint on the atmospheric composition resulting in numerous potential outcomes of element abundance ratios. Various studies focus on understanding the role of the snowline on the carbon to oxygen ratios in hot Jupiters (e.g., Öberg et al., 2011; Piso et al., 2015; Ali-Dib, 2017). Objects formed inside the water ice line are expected to have a similar C/O ratio to that of a star. Objects formed beyond the water ice line but inside the CO_2 ice line where gas is carbon-rich but oxygen-poor are expected to have a super-stellar C/O ratio. Object farther away from host stars between the CO_2 ice line and CO ice line, where even more oxygen condense compared to carbon, have further enhanced the C/O ratio. Finally, objects formed through gravitational instability are also expected to have the stellar C/O ratio as all material is mixed. C/O ratio of several exoplanets was studied and reported (e.g., Madhusudhan et al., 2011; Line et al., 2021). Madhusudhan et al. (2011) found a super-stellar C/O ratio for WASP-12b, which can be explained by gas accretion between the water and CO ice lines. Line et al. (2021) found sub-stellar/solar abundances of C and O and a $\sim$solar C/O ratio for WASP-77Ab. Hence, the possible formation scenario could be that the core accreted its atmosphere inside the water ice line. Many planets with measured C/O ratios would shred more light to the formation of SSOs.

A large sample with well-characterised systems is needed to obtain a deep insight into the formation and evolution of SSOs. Here space-based photometric survey missions play a crucial role in characterising transiting SSOs. This was shown by discoveries from the CoRoT mission (Auvergne et al., 2009) and the Kepler/K2 missions (Borucki et al., 2010), and currently, all discoveries are from the TESS mission (Ricker et al., 2015). TESS has become an invaluable resource in delivering new transiting SSOs. However, in contrast to previous missions, TESS has the advantage of observing many bright stars making new candidates more accessible to spectroscopic follow-up. Given that SSOs produce relatively deep transits around the main-sequence stars and relatively large RV signals, they can be easily studied with moderate-precision RV campaigns. Available space mission photometry, spectroscopic follow-up observations and Gaia astrometric data (Gaia Collaboration et al., 2018, 2021) create synergy in characterising transiting SSOs.

As was mentioned before, the precise measurement of the mass, radius and age of SSOs is crucial to revealing their formation and evolution. However, the precision of these key parameters is limited by our knowledge of the same properties

for the host star, especially the age. Tremendous effort has been made to precisely constrain stellar parameters. Such efforts include space-based missions to measure the distance to stars through their parallax, directly observing the stellar angular diameter through interferometry, analysing high-precision space-based photometry for asteroseismic signals, analysing high-resolution spectra through equivalent width calculations, spectral synthesis, or other techniques, or by comparing the shape of the spectral energy distribution (SED) from different photometric observations to those of synthetic stellar atmospheric models. Furthermore, estimating a precise age for an isolated field star is one of the most challenging tasks in astronomy (e.g., Soderblom, 2010). The available methods include stellar isochrone fitting, gyrochronology analysis, R'_{HK} index, lithium equivalent width (EW_{Li}), X-ray luminosity, or membership in young associations.

Finally, to understand the formation and evolution of these systems, one needs to understand the effect of other bodies on the transiting SSOs. Planets can be significantly affected by wide companions through different processes, such as gravitational instability, accretion, velocities of colliding planetesimals, dissipation, or Lidov-Kozai effects (e.g., Boss, 2006; Nelson, 2003; Moriwaki and Nakagawa, 2004). If we look at multiple stellar systems with planets, possible peculiarities in parameter distributions of inner planets were searched by many teams (e.g., Eggenberger et al., 2004; Desidera and Barbieri, 2007; Fontanive and Bardalez Gagliuffi, 2021). To highligh some results, Eggenberger et al. (2004); Desidera and Barbieri (2007); Fontanive and Bardalez Gagliuffi (2021) observed that the most massive short-period planets are found primarily in systems of tight binaries, or Fontanive and Bardalez Gagliuffi (2021) found that more massive planet-host stars are more often in multi-stellar systems, and that the mass of the stellar companions has no significant effect on planetary properties.

Aims

The aim of this thesis is the detection and characterisation of transiting BDs and EGPs. We use various techniques to determine stellar mass, radius and age, which are crucial to derive the parameters of a companion and discuss its formation and evolution. Furthermore, we can study tidal interactions between the companion and the host star for each system, which provide additional methods to constrain the formation. Ultimately, this research will have the greatest impact on understanding the formation mechanisms of SSOs with the characterisation of more systems like these. Once the TESS mission started operations, we observed a rapid growth of transiting SSOs beyond our expectations which radii and often also masses are measured with great precision. With such data, we can expect to better understand the formation and evolution of individual SSOs in the upcoming years. However, as many stars are part of multi-stellar systems, it is also important to understand interactions between wide companions and inner planets, which can cause peculiarities in their parameter distributions. The study of such peculiarities is another aim of this thesis.

Chapter 1 presents the current knowledge on BDs and EGPs, followed by a description of various techniques that can be used to precisely determine stellar parameters. Chapter 2 presents an introduction to the theory of tidal interactions. Chapters $3-5$ present three papers which I led as part of several international collaborations. Specifically, chapter 3 presents the discovery of the first transiting BD from the TESS space mission (Šubjak et al., 2020). We showed that the host star is a metallic-line A-type star, an Am star, which makes TOI-503b the first brown dwarf found around such a stellar type. This work also discusses tidal interactions between a brown dwarf and a host star and uses brown dwarf parameters to test substellar evolution models. These are the results of a global collaboration among the KESPRINT consortium, Harvard University and Physical Research Laboratory, India. Chapter 4 presents the discovery of the youngest transiting Saturn-mass planet (Šubjak et al., 2022). The work explores various stellar age-dating techniques and discusses what we can learn from tidal interactions even though the planet is not massive enough to be expected to have formed by gravitational instability. Particularly interesting is that TOI-1268b has mass and radius similar to that of Saturn, despite the much younger age between $110-380$ Myr. These are the results of a global collaboration among the KESPRINT consortium. Chapter 5 presents the search for planets in systems with wide BD companions. The work also compares parameter distributions of planets around single stars, planets around stellar binaries and planets in systems with wide BD companions to study how wide BD companions affect planetary systems. These are the results of a global collaboration with astronomers from Instituto de Astrofíısica de Canarias. Finally, Chapter 6 summarises the main results and conclusions of this thesis.

1. Introduction

This section presents the current knowledge on BDs and EGPs, followed by a description of various techniques that can be used to precisely determine stellar parameters. The precision of stellar parameters is crucial not only for the characterisation of their companions but also for studying tidal interactions between a companion and a host star. It is partly based on my publication Šubjak et al. (2022).

1.1 Brown dwarfs

Brown dwarfs (BDs) form a group of objects separating giant planets from low-mass stars. The exact definition is based on the mass, as electron degeneracy pressure in the interior of BDs causes them to have a similar radius as giant planets. The lower edge of the mass range is 11–16 Jupiter masses (M_J), which is a condition to sustain deuterium fusion (Spiegel et al., 2011). The upper end is then at 75–80 M_J (Baraffe et al., 2002) which creates conditions capable of supporting hydrogen fusion, typical for stars. These intervals reflect the sensitivity to the metallicity and the chemical composition of BDs. Recently this definition has been increasingly questioned (e.g., Whitworth, 2018; Hatzes and Rauer, 2015; Persson et al., 2019), and the classification of objects close to these boundaries are blurred by insufficient precision on the derived parameters (Díaz et al., 2014; Zhou et al., 2019).

The discovery of the first two BDs, Teide 1 and Gliese 229B (Rebolo et al., 1995; Nakajima et al., 1995), were announced in 1995. Since then, the study of BDs has gone through rapid development. Thousands of BDs have been discovered so far; many come from all-sky infrared surveys (e.g., Lodieu et al., 2007; Pinfield et al., 2008; Metchev et al., 2008; Burningham et al., 2010; Kirkpatrick et al., 2011; Cushing et al., 2011; Lodieu et al., 2012; Carnero Rosell et al., 2019; Kirkpatrick et al., 2021), such as the Two-Micron All-Sky Survey (2MASS; Skrutskie et al., 2006), the Wide-field Infrared Survey Explorer (WISE; Wright et al., 2010), the Deep Near-Infrared Survey of the Southern Sky (DENIS; Epchtein et al., 1997), the UKIRT Infrared Deep Sky Survey (UKIDSS; Lawrence et al., 2007), and the VISTA Hemisphere Survey (VHS; McMahon et al., 2013). Additional discoveries come from large-scale optical surveys (e.g., Hawley et al., 2002; Metchev et al., 2008; Deacon et al., 2011, 2014; Carnero Rosell et al., 2019), such as the Dark Energy Survey (DES; Abbott et al., 2018), the Sloan Digital Sky Survey (SDSS; York et al., 2000), and the Panoramic Survey Telescope and Rapid Response System (Pan-STARRS; Chambers et al., 2016). These usually isolated brown dwarfs have traditionally been identified via their colours as their spectral energy distribution peaks in the near-infrared.

Several works focus on the study of the initial mass function (IMF) of BDs (e.g., Luhman, 2004; Bayo et al., 2011; Scholz et al., 2012, 2013; Mužić et al., 2015, 2017). Mužić et al. (2017) used the high-resolution adaptive optics data of the young (~ 1 Myr) dense cluster RCW 38 obtained with the NACO instrument at the Very Large Telescope. They found a star/BD ratio between two

and five, which is consistent with the previous works of other young star-forming regions (e.g., Slesnick et al., 2004; Levine et al., 2006; Luhman, 2007) as well as with the estimate of the star/BD ratio in the field (Bihain and Scholz, 2016). They estimated that the Milky Way galaxy contains between 25 and 100 billion brown dwarfs. Furthermore, their results do not show evidence that a high stellar density affects the formation efficiency of brown dwarfs and very-low-mass stars. These works suggest that BDs are indeed common objects. However, Thies et al. (2015) pointed out the inconsistency with the theory in that formation of BDs by direct cloud fragmentation similar to stars has problems reproducing such a large amount of observed BDs. The reason is that this process rarely produces BDs as it requires specific conditions such as a high-density, gravitationally self-bound cloud but very low mass so that the object does not accrete enough mass to become a star (Adams and Fatuzzo, 1996). The observed IMF contains too many brown dwarfs compared to what is predicted by theory (Padoan and Nordlund, 2002; Hennebelle, 2018). This inconsistency can be seen in Figure 1.1. Hennebelle and Chabrier (2008) proposed that this deficit might be solved by including turbulent fragmentation descriptions in their models; however, others interpret this inconsistency as a sign that an additional formation channel is needed to match the observations.

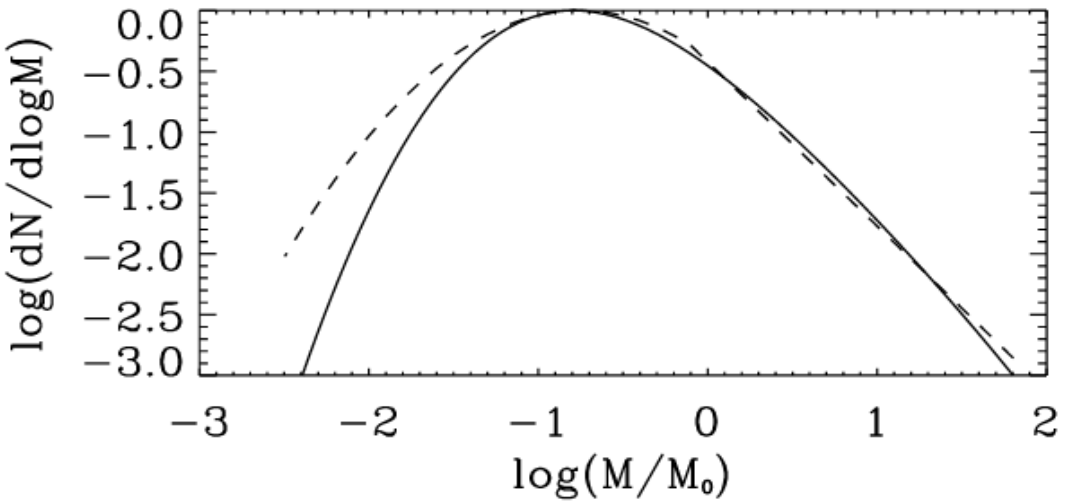

Figure 1.1: Comparison between the theoretical IMF (solid line), and stellar/brown dwarf system IMF representative of the Galactic field and young clusters (dotted line) (Chabrier, 2003). The bottom axis is in units of solar masses. We can see that the theoretical model does not reproduce the observed abundance of brown dwarfs with $M \leq 0.08\,M_{\odot}$. Source: Hennebelle and Chabrier (2008).

To discuss if BDs are typically formed like stars, we can study their binarity fraction. Most stars are formed as multi-stellar systems. Goodwin and Kroupa (2005) discusses that the dynamical decay of systems with three and more stars would result in a large population of single stars that are not seen in the young stellar populations with high binary fractions (Duchêne, 1999). This leads to a strong constraint on star formation theories that formation processes must typically produce only 2 or 3 stars. Oppositely, we observe only a small fraction of star-BD binaries, the so-called *brown dwarf desert* (e.g., Grether and Lineweaver,

2006; Sahlmann et al., 2011) and also small number of a BD-BD binaries (e.g., Bouy et al., 2003; Burgasser et al., 2003). However, the low number of brown dwarf binaries can also reflect the decrease in binarity fraction in dependence on primary mass as observed for stars. Furthermore, poor constraints of the BD binary fraction at small separations from photometric surveys lead to uncertainties in binarity estimations (Bardalez Gagliuffi et al., 2014). However, these may still indicate that most BDs do not form like stars. These can also be seen in the primary mass vs mass ratio diagram of binaries from the Chamaeleon I star-forming region presented in Lafrenière et al. (2008). Thies and Kroupa (2008) showed that the observed binaries could be reproduced by random pairing from the IMF, however, only when treating BDs and stars as separate populations (see Figure 1.2). Furthermore, Thies and Kroupa (2007) also discussed that the distribution of semi-major axis in stellar binaries is different than in the case of BD binaries which have a much narrow range.

Thies et al. (2010) studied the effects of stellar encounters in embedded clusters on the circumstellar disks. They observed that after the passage of the perturbing star, tidal arms are formed in the circumstellar disks, and part of the mass is transferred to the passing star. In these tidal arms, gravitational instabilities form bound objects, typically between 100 and 200 au from the star. Each simulation typically produces between two and five low-mass objects with masses between those of very massive planets and very low-mass stars. Some of these objects fall into the central star, and some are ejected, typically with a mass of a brown dwarf. The rest continue to accrete material and becomes stars. The authors found that the IMF of brown dwarfs produced in the simulations is comparable with the IMF from star clusters (Thies and Kroupa, 2007). Furthermore, models predict that around 15% brown dwarf binaries are formed, which is also consistent with observations (Burgasser et al., 2010). Basu and Vorobyov (2012) computed formation and evolution of protostellar disk in which gaseous clumps are formed by disk fragmentation and often are ejected due to gravitational interactions with other gaseous clumps, gas disk and with host star. Furthermore, they found that these clumps do not need to reach stellar density to be ejected and that they can be tidally disrupted during the ejection process. Clumps that survive ejection can cool down and contract to form BDs with an accretion disk. Hence, observations of BDs with accretion disks, which were previously used to favour the formation through the direct collapse of molecular cloud (Luhman, 2007), can also be the results of the disk fragmentation. (Vorobyov, 2016) found that only gaseous clumps with a mass larger than $20\,M_J$ can survive ejection and that the ejection of the most massive clumps can cause fragmentation to BD binaries. Furthermore, the structure of pre-BD cores would differ from that expected formed via molecular cloud fragmentation. It can be used to distinguish between formation scenarios. In conclusion, there are expected two different formation chains for free-floating BDs: star-like formation and disk fragmentation with subsequent dynamical evolution. Marks et al. (2017) discussed the question of how to distinguish between these formation scenarios observationally. They showed that binary fraction as a function of primary mass contains specific features that can be used to distinguish in which way most of BDs formed.

We also observe the rapid rising of discoveries of transiting BDs (e.g., Persson et al., 2019; Šubjak et al., 2020; Carmichael et al., 2020, 2021; Palle et al., 2021)

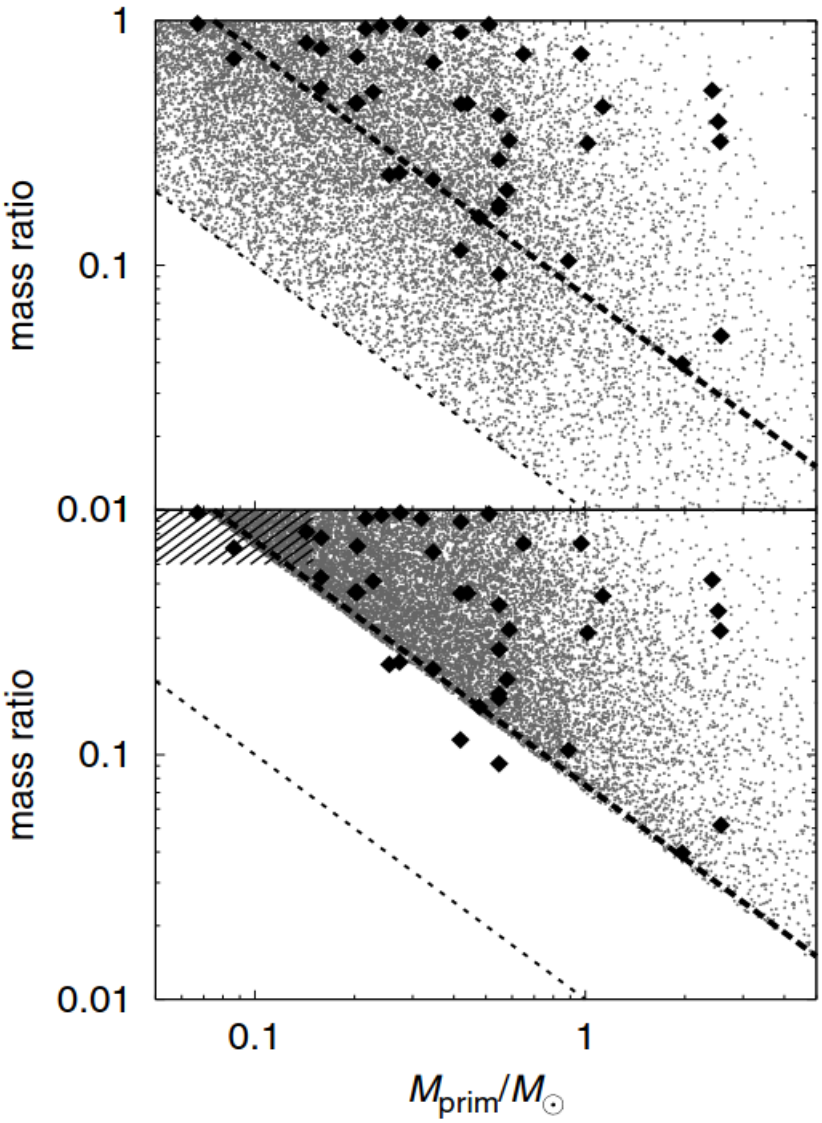

Figure 1.2: Mass-ratio vs primary mass distribution. Upper panel: Binaries formed by random pairing over the complete mass range of a single population of BDs and stars (grey points) and the observations of the Chamaeleon I star-forming region (black diamonds) (Lafrenière et al., 2008). Lower panel: Binaries formed by random pairing of stars with $M_{\star}$ above 0.075. If the binaries were formed by random pairing over the complete mass range of a single population of BDs and stars, we would observe lower mass ratios. The observations agree well with a random pairing of stars as the separate population. Source: Thies and Kroupa (2008)

mainly thanks to space missions such as the CoRoT mission (Auvergne et al., 2009), the Kepler/K2 mission (Borucki et al., 2010), and currently the TESS mission (Ricker et al., 2015). These objects are thought to form either in-situ via gravitational instability or via core accretion at larger distances from host stars. The fact that brown dwarfs form relatively rarely close binaries with stars (e.g., Vogt et al., 2002; Patel et al., 2007; Sahlmann et al., 2011; Nielsen et al., 2019) suggests that they are not the main products of these processes. To observation-

ally constrain the formation path of individual systems, they need to be precisely characterised. In such binary systems, the primary stars come in handy. If we assume that both components formed in the same environment under the same conditions, such bodies will share common properties (e.g., age and metallicity), which can be derived for one of them and applied to the other (Faherty et al., 2010). For close binary systems, we can also measure the precisely the mass by measuring the radial velocities of host stars. Furthermore, if a BD is transiting, we can measure its radius precisely. We can then use this information to test up-to-date structure, evolution, and formation models, which still contain many uncertainties. So far, we observe a similar number of transiting BDs around low-mass M stars, G-type and F-type stars (27±13% of the population for M stars, 22±11% for G stars and 32±15% for F stars) and a decrease in numbers around K-type and A-type stars (8±6% of the population for K stars and 11±7% for A stars) (see Figure 1.3). With the increasing number of transiting BDs, we will be able to better constrain the distribution of transiting BDs around individual spectral types to understand how stellar properties influence both formation processes. Damiani and Díaz (2016) argue that tidal interactions with the host star and angular momentum loss through magnetic braking can lead to the inward migration of BDs with the BD being engulfed by its parent star. This process should also be considered to influence observed fractions as its timescale is longer for brown dwarfs orbiting smaller stars.

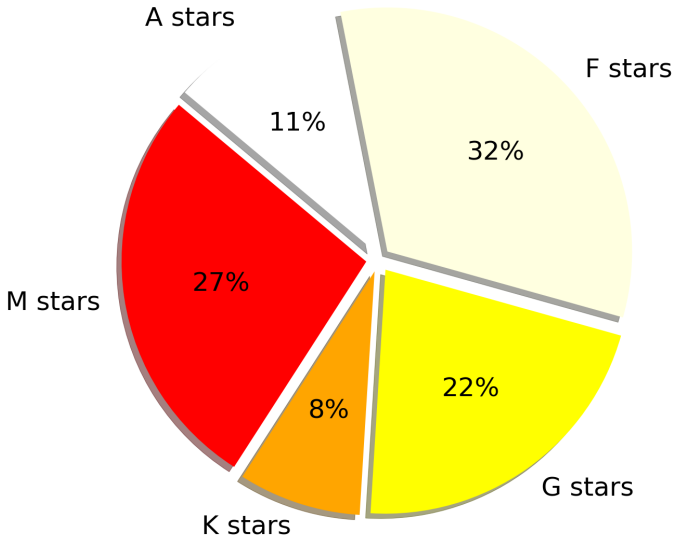

Figure 1.3: Percentage of the currently known transiting BDs vs spectral type of host star.

1.2 Giant planets

According to the classical picture, giant planets form from planetary cores made of ices and rocks that grew beyond a critical mass of about ten times the mass of the Earth, at which point they began accreting hydrogen and helium and increased their mass rapidly (Perri and Cameron, 1974; Mizuno, 1980; Bodenheimer and Pollack, 1986). The first EGP discovered around a solar-type star, 51 Pegasi b

(Mayor and Queloz, 1995) is a hot Jupiter with an orbital period of ~ 4 days much different from what we see in our solar system. Indeed, it was the first hint of how diverse the planetary systems are and that many processes need to be involved in understanding the general concept of planetary formation.

Studying the parameter distributions of known gas giants provides key evidence about their formation and evolution. The radial distribution of gas giants follows a bimodal shape with the first peak between 0.04 and 0.05 au representing the group of hot Jupiters and the second peak observed at larger separations between $1 - 4$ au (see Figure 1.4). The eccentricity of planets has a rising trend towards larger separations as tidal interactions with a host star would circularise close planets. However, planet-planet scattering is an important effect, enhancing the eccentricities. Raymond et al. (2009) presents a study of the planetary system's architecture that evolves under the combined effects of planet-planet and planetesimal scattering. The very important result derived from the eccentricity distribution is that to be able to match the observed eccentricity distribution, $\sim 75 - 95\%$ of giant exoplanets systems need to be survivors of the instability process between two planets (Jurić and Tremaine, 2008; Chatterjee et al., 2008; Raymond et al., 2010). Another important property found is the correlation between the gas giant fraction and the metallicity of the host stars. Stars with higher metallicity host more giant planets (Santos et al., 2003; Fischer and Valenti, 2005; Johnson et al., 2010) (see Figure 1.5). Johnson et al. (2007) discussed the correlation between the gas giant occurrence rate vs stellar mass for distances below 2.5 au. Ghezzi et al. (2018) later quantified that the occurrence rate is proportional to mass of star with exponent gamma equal 1.05 ($M_\star^\gamma$; $\gamma = 1.05 \pm 0.28$). Nielsen et al. (2019) found a similar correlation for planets at wide separations ($10 - 100$ au) using data from the Gemini Planet Imager. In comparison to giant planets, BDs show a different distribution of orbital distances, with an occurrence rate around 1%, independently of the stellar host mass. It suggests that giant planets and BDs should be treated as different populations similarly as in the case of BDs and stars.

The formation of giant planets through core accretion consists of several phases. Firstly, planetesimals are formed by pebbles' accretion. Secondly, the relatively long phase of slow gas accretion begins when the planetesimals are sufficiently massive. When the mass of gas is similar to the mass of a core, the runaway accretion phase is triggered, and planets accrete a lot of mass in a short time (Pollack et al., 1996). These processes are closely connected to the migration processes. Johansen and Lambrechts (2017) presents the growth tracks of planetary mass versus semimajor axis for all the major classes of planets. These tracks show that planetesimals formed at separations smaller than a few au migrate very close to a star and end up as hot Jupiters, while, for example, planetesimals formed at ~ 15 au end up at ~ 5 au. Hence, there are several theories for the formation place of Jupiter. Either Jupiter's planetesimal formed at a large distance from Sun, or it could form a bit closer and migrate slower (Bitsch et al., 2019). Another possibility is that Jupiter alone would migrate much closer toward the Sun, but Saturn stops such migration, and both planets experienced a reverse migration (Masset and Snellgrove, 2001).

Giant planets' formation and migration strongly influence planetary systems, as in the case of our Solar system. It is clear that Jupiter and Saturn affected

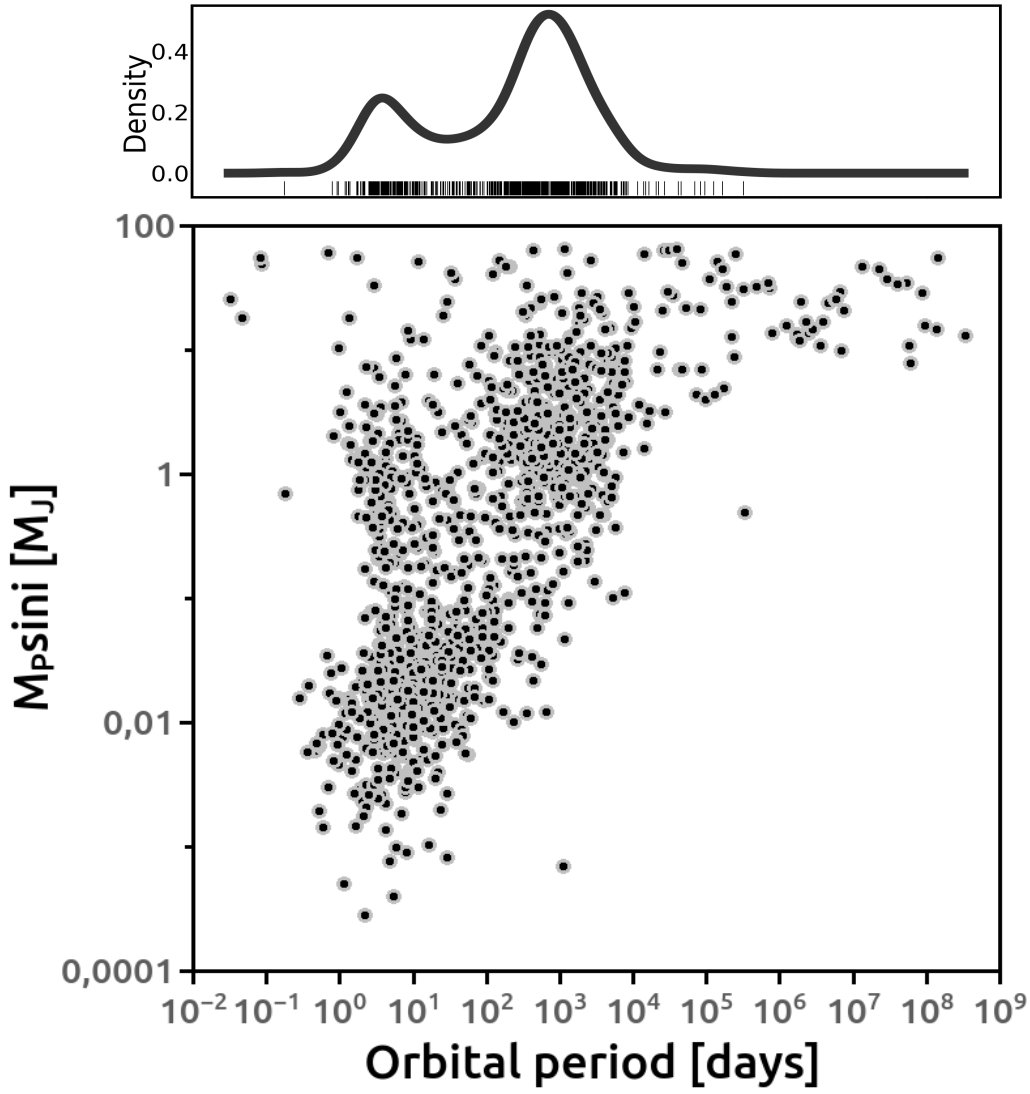

Figure 1.4: Planetary minimum mass versus orbital period for the known planets characterised by radial velocity. In the top panel, we can see the kernel density estimate of planetary orbital periods for the mass range of Jovian planets between 0.1 and 15 M_J revealing the bimodal distribution. Data from Fontanive and Bardalez Gagliuffi (2021).

the inner planets' orbits and masses; however, it was also shown that Jupiter affected the amount of water on the terrestrial planets (Morbidelli et al., 2016). Previous studies have discussed the role of giant planet formation and migration on the planetary systems. They predicted compact systems composed of inner super-Earths/mini-Neptunes and hot Jupiters (e.g., Fogg and Nelson, 2005, 2007; Raymond et al., 2006; Mandell et al., 2007). A few such systems were indeed discovered (Becker et al., 2015; Cañas et al., 2019; Huang et al., 2020). Furthermore, Raymond et al. (2006) and Mandell et al. (2007) discussed that in systems with a hot Jupiter, Earth-mass planets are often formed within the habitable zone. However, these planets would accrete much more water in comparison to planets in systems with distant giant companions similar to our Solar system. The reason is that distant EGPs, when they are massive enough, prevent the migration of icy

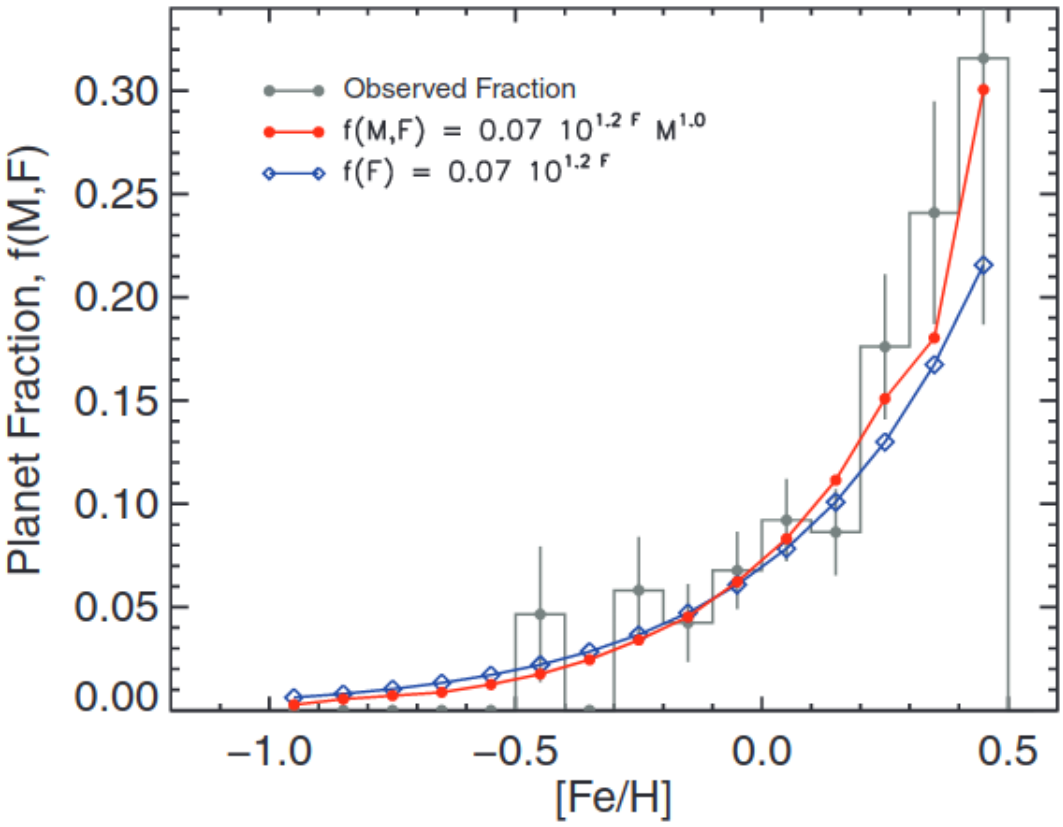

Figure 1.5: Planet fraction ($N_{planets}/N_{stars}$) as a function of stellar metallicity for the sample of 1266 stars drawn from the California Planet Survey (gray histogram) (Johnson et al., 2010). The filled red circles represent the median planet fraction of the stars in each bin. The blue diamonds represent the planet fraction for solar-like stars. Source: Johnson et al. (2010).

pebbles to the inner part of the disk (Morbidelli et al., 2016). Planets in systems with an inner EGP contain about twenty times as much water as those formed in outer EGPs simulations (Raymond et al., 2006). Hence, we can imagine these planets as water worlds with thick global oceans. None of such systems has been detected so far; however, these predictions make systems with hot Jupiters good targets for future missions focusing on the detection of planets in the habitable zone around solar-like stars, such as PLATO (Rauer et al., 2014).

1.3 Stellar parameters

The accurate knowledge of stellar parameters is fundamental to understanding their formation and evolution, as well as the formation and evolution of their companions. However, it can also tell us a lot about the formation and evolution of galaxies as stars represent building blocks. Hence, it is important to derive these parameters precisely, preferably without using theoretical assumptions. Precisely measuring stellar parameters is one of the most challenging tasks in astronomy.

1.3.1 Mass and radius

The mass and radius, together with luminosity and chemical composition, can be considered the first-order parameters describing the physical properties of stars. These parameters are key ingredients of models of stellar structure and evolution. Other parameters such as effective temperature or surface gravity can be derived from them. Every astrophysical application requires a different mass and radius precision, although we always try to reach a best possible precision. Testing different stellar structure and evolution models is one of the most demanding tasks, usually requiring precision of $\sim 1-3\%$. Another application demanding great precision is the study of exoplanets. An exoplanet's mass derived through the radial velocity method depends on the host star's mass. Similarly, we can derive only the ratio between planetary and stellar radius from transit photometry. Hence the precision on the exoplanet mass and radius is limited by the precision on the stellar parameters. Unfortunately, there are only a few methods to measure stellar mass and radius directly, and these methods are not applicable uniformly across the Hertzsprung–Russell (H–R) diagram.

- One method considers eclipsing binaries to measure mass and radius very precisely. These parameters depend primarily on the system's geometry through the analysis of the light curves and on Newtonian mechanics through measuring radial velocities. Torres et al. (2010) has shown that eclipsing binaries can achieve precision in mass and radius measurements of $2-3\%$.

- Another method to precisely measure stellar mass and radius is asteroseismology, the study of stellar oscillations (e.g., Brown and Gilliland, 1994; Christensen-Dalsgaard, 2004; Aerts et al., 2010; Gilliland et al., 2010). The precision of space-based photometry has enabled the detection of stellar acoustic modes, which allows precision in mass and radius measurements of a few per cent (e.g., Bruntt et al., 2012; Huber et al., 2013). However, as the amplitude of these modes scales with the stellar size, asteroseismology can usually be used only on solar-like or larger stars where the observations are not complicated by stellar activity or photometric noise.

- In the case of stellar radii, we must also add interferometry to the list. Optical and infrared interferometry has been used several times to measure the stellar angular size directly (e.g., Berger et al., 2006; von Braun et al., 2014). However, one needs to know the precise parallax to determine the stellar radius, and this method can be used only on relatively close and bright stars. Hence, low-massive cold stars are usually undersampled as they are faint.

Serenelli et al. (2021) provides the summary of available techniques for stellar mass determination across stars of different evolutionary stages. They also provide a list of more than 200 stars with precise mass measurements below 2%. 75% of these stars are main sequence stars, and the rest covers all other evolved stages. As these techniques summarised here are not applicable to all stars, we usually rely on models of stellar interiors and atmospheres to measure the stellar properties of isolated field stars. Serenelli et al. (2021) compares the stellar

radius measured from asteroseismology with that measured from spectral energy distribution in combination with parallax and found a good agreement between both methods, with a typical scatter of $\sim 10\%$.

Spectral synthesis and stellar isochrones

Spectroscopic analysis is one way how to determine stellar parameters, such as the effective temperature $T_{\rm eff}$, surface gravity $\log g$, metallicity [Fe/H], and the projected stellar equatorial velocity $v \sin i$, by comparing observed spectra with synthetic ones. To perform such analysis in the next sections, we used the `iSpec` interface (Blanco-Cuaresma et al., 2014; Blanco-Cuaresma, 2019). `iSpec` combines several synthetic programs to generate synthetic spectra for stellar parameters grids: SPECTRUM (Gray, 1999), TURBOSPECTRUM (Plez, 2012), SME spectral synthesis (Valenti and Piskunov, 1996; Piskunov and Valenti, 2017), MOOG (Sneden et al., 2012) and SYNTHE (Kurucz, 1993). These synthetic spectra are then compared to the observed one, and the spectral fitting technique minimises the χ^2 value between them by executing a nonlinear least-squares (Levenberg-Marquardt) fitting algorithm (Markwardt, 2009). Specifically, we are using `SME` together with the MARCS models of atmospheres (transformed to the format that `SME` requires) (Gustafsson et al., 2008), and version 5 of the GES atomic line list (Heiter et al., 2015). The MARCS models cover effective temperatures from 2500 to 8000 K, surface gravities from 0.00 to 5.00 dex, and metallicities from -5.00 to 1.00 dex, and the GES line list spans over the interval from 420 to 920 nm and includes 35 chemical species. Brewer et al. (2015) compared surface gravity measurements from spectroscopic analysis with `SME` with asteroseismological measurements and found a good agreement.

One technique for determining stellar parameters is to compare larger parts of observed spectra to synthetic ones. However, one should carefully consider which regions are suitable for such analysis. Yee et al. (2017) used eight 100 Å intervals between $5000-5800$ Å and derived the final parameters by averaging values from all intervals, which gives relatively good results. However, in this technique, parameter determination is complicated by having to fit several parameters at the same time. When one parameter is mismatched, the others are affected by systematic errors. Another technique discussed in Fridlund et al. (2017) uses specific features in the spectrum sensitive to individual stellar parameters. We can use the wings of Hα line (Cayrel et al., 2011) to determine the effective temperature. Furthermore, we need to exclude the core of this line as it originates in the chromosphere and would incorrectly result in higher temperatures. However, such temperature depends on how large the part of the Hα line we exclude and also how well the continuum is normalised. To determine a metallicity and projected stellar equatorial velocity, we can use a large number of Fe I,II lines in the region between 5970 and 6430 Å.

The stellar parameters derived from spectroscopic analysis, together with photometric and astrometric data, can then be used to derive a mass, radius, or age when compared with models mapping the stellar evolution. Several such models are available and widely used in the literature: the PARSEC isochrones (Bressan et al., 2012), the MIST isochrones (Choi et al., 2016), the Dartmouth isochrones (Dotter et al., 2008), the Geneva isochrones (Lejeune and Schaerer, 2001), or the Brussels isochrones (Siess et al., 2000).

SED analysis

Another method to determine the parameters of stars is to compare the shape of the spectral energy distribution (SED) to theoretical models of the stellar atmosphere. The stellar atmosphere represents the link between the observations and models of stellar structure and evolution, and the SED represents the robust prediction of atmospheric properties. Even for the cool stars, whose spectra are affected by convective motions and turbulent flows, Chiavassa et al. (2018) discussed that using realistic 3D hydrodynamical stellar atmosphere simulations does not cause larger changes than 5% in comparison to classical 1D hydrostatic models for late-type stars. As the SED shape, which can be mapped by photometric observations in different wavelength bands, depends in first order on the radiative flux of the bottom parts of the stellar photosphere, it can be used as a good thermometer. In the second order, the SED shape is influenced by lines and continuous opacity; hence it can also be useful for predicting the surface gravity and chemical abundances.

One of the most used approaches is to minimize the χ^2 function between the SED shape from available photometric measurements and different atmospheric models. In the next chapters we used the Virtual Observatory SED Analyser (`VOSA`; Bayo et al., 2008) to model the SED of stars. `VOSA` uses grids of different models, from that we used: BT-Settl-AGSS2009 (Barber et al., 2006; Asplund et al., 2009; Allard et al., 2012), BT-Settl-CIFIST (Barber et al., 2006; Caffau et al., 2011; Allard et al., 2012), BT-NextGen GNS93 (Grevesse et al., 1993; Barber et al., 2006; Allard et al., 2012), BT-NextGen AGSS2009 (Barber et al., 2006; Asplund et al., 2009; Allard et al., 2012), and Coelho Synthetic stellar library (Coelho, 2014). To obtain available photometry `VOSA` enables access to different photometric tables. We used some of the most common photometric surveys and their filters spanning the wavelength range 0.4 – 22 μm: 2MASS J, H, K bands (Cutri et al., 2003), WISE $W1-4$ bands(Cutri et al., 2021), Tycho B, V bands (Høg et al., 2000), Gaia DR2/3 G, B_P, R_P bands (Gaia Collaboration et al., 2018, 2021), Strömgren-Crawford u, v, b, y bands (Paunzen, 2015) or AKARI bands (Ishihara et al., 2010). `VOSA` also enables the calculation of the stellar reddening caused by interstellar dust. Based on the model with the minimal χ^2 function, `VOSA` determines an effective temperature $T_{\rm eff}$, surface gravity $\log g$, and metallicity [Fe/H]. The available photometry is used to determine a total observed flux, which is translated using star distances (typically from Gaia DR3) into a bolometric luminosity. An effective temperature and bolometric luminosity are then used to determine stellar radius via the Stefan–Boltzmann law. Additionally, an effective temperature $T_{\rm eff}$, surface gravity $\log g$, and metallicity can be used to determine the mass, radius and age when compared to stellar isochrones, similarly as in the previous section. Finally, `VOSA` enables to compare the stellar SED with those in template collections to determine a spectral type. We used the template collections provided by Kesseli et al. (2017).

1.3.2 Age

Unlike mass and radius, stellar age cannot be measured directly, but can only be estimated through different age-dating techniques. Only one star has precisely and accurately determined its age, and it is the Sun. However, even the Sun

itself does not reveal its age which we determined from the material in the solar system. This main obstacle makes age the most difficult stellar property to derive. Furthermore, because stars are evolving, we need a reliable way to measure their age to understand many physical phenomena. Barnes (2007b) has discussed which attributes a perfect age indicator should fulfil. Such an age indicator should be well-defined and applicable for a single star but should provide the same ages for all stars when used on an coeval sample. Furthermore, such an indicator should be sensitive only to age, and its physics should be well understood with the least possible assumptions.

Now it is clear that such an age indicator does not exist, and usually, we need to settle for less, often much less. Each age indicator is affected by many underlying phenomena; hence, these activity indicators may disagree in some cases. However, in many cases, using more activity indicators is sufficient to provide reliable constraints on age. These age indicators are often studied on stellar clusters; however, open clusters older than one Gyr are sporadic and tend to be distant. Another obstacle is that stellar parameters do not dramatically change during the main-sequence phase. Hence, only for young systems or, on the contrary, for old systems after the main-sequence phase, we can get reliable age constraints. In summary, each interval of stellar age and spectral type presents its problems and has its relevant activity indicators.

Stellar isochrones

One of the methods available for stellar age determinations, which is particularly important in observational studies, is isochrone fitting. As previously mentioned, it compares stellar parameters derived from the spectroscopic or SED analysis, together with photometric and astrometric data, to theoretical stellar evolutionary sequences.

Isochrone fitting can provide relatively accurate ages; however usually not very precise. It is a useful technique to determine the ages of stellar associations, observing the minimum mass of stars which left the main sequence (MS). However, in some cases, it can also be used on single stars. Age is difficult to measure, particularly for low-mass (G,K,M) stars on the MS. The uncertainties can be as large as the universe's age for these stars. This is caused by the fact that while a star is sitting on the MS, its physical properties do not change rapidly. It can be seen in the space between different tracks on the H-R diagram. They are very closely spaced, and many of them (usually in the range of several Gyr) lie in typical observational uncertainties for luminosity and effective temperature (or absolute magnitude vs colour) in Figure 1.6. Different cases are stars which already left the MS. Here, the spacing between tracks is much less dense, and the precise measurement of input parameters would lead to a very precise age.

Gyrochronology

The slowing down of the rotation period of main sequence stars through magnetic braking was first reported by Skumanich (1972), who observed young clusters and moving groups, such as Pleiades, Ursa Major, or Hyades. He defined the Skumanich law according to which stellar rotation slows down with the square root of time. Then, Barnes (2003) proposed to use such age-rotation dependency

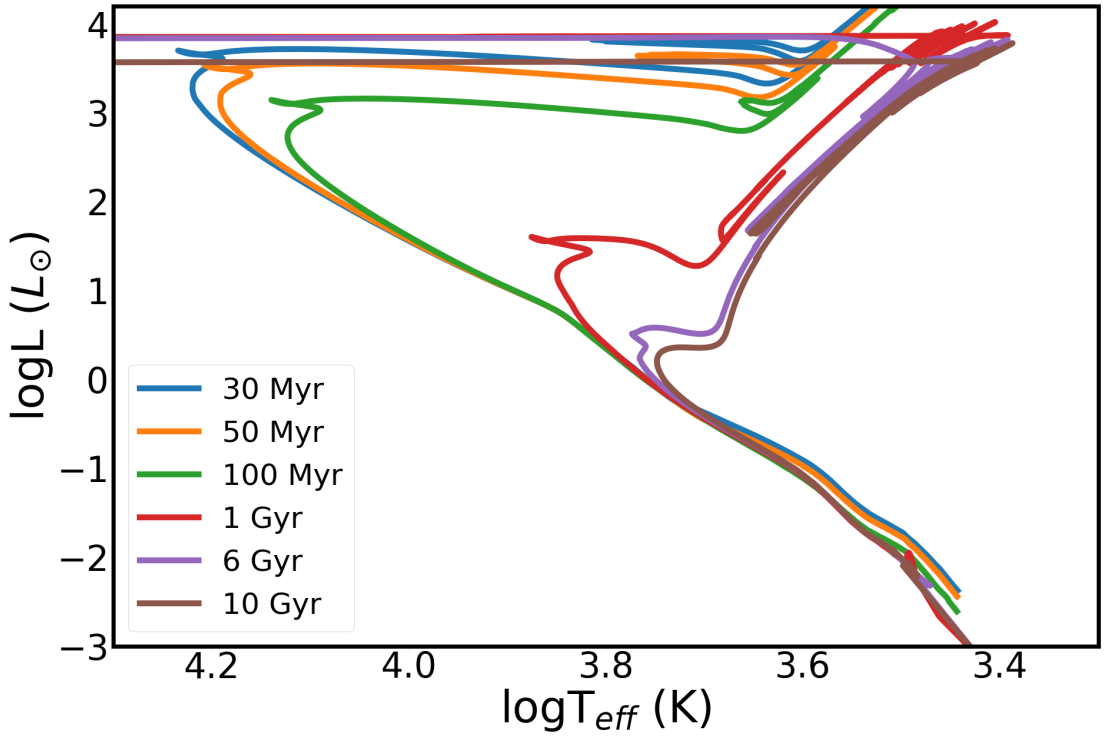

Figure 1.6: Luminosity vs effective temperature plot. Curves represent MIST isochrones for ages: 30 Myr (blue), 50 Myr (orange), 100 Myr (green), 1 Gyr (red), 6 Gyr (purple), 10 Gyr (brown).

as a clock to measure the age of stars, termed gyrochronology. Meibom et al. (2009) discussed that F and G stars in the M35 cluster (∼150 Myr; Meibom et al., 2009) behave pretty much as Skumanich law predicts comparing to Hyades cluster (∼650 Myr; Soderblom et al., 1993a), while for K dwarfs, the law predicts a faster spin-down rate than observed. Meibom et al. (2011) and Cargile et al. (2014) found similar behavior looking at the NGC 6811 (∼1 Gyr; Curtis et al., 2019), and Blanco 1 clusters (∼130 Myr; Cargile et al., 2010). These authors discuss two different sequences observed in these clusters and that the rate of transition between them is inversely related to the stellar mass.

Epstein and Pinsonneault (2014) discussed two sources of uncertainties that complicate the measurement of stellar age: the range of initial stellar rotation periods and latitudinal surface differential rotation. However, the convenient characteristic of stars that allows their ages to be inferred from their current rotation periods and independently of their primordial ones comes from the steep dependence of the spin-down rate on rotation period (Kawaler, 1989). Stars spinning with high angular velocity will experience a much greater angular momentum loss rate than slowly spinning stars, and for this reason, no matter the initial rotation period, solar-type stars will have the same rotation period after around the age of the Hyades, 500–700 million years (Irwin and Bouvier, 2009; Gallet and Bouvier, 2015). After this time, the age of a star can be inferred, to first order, from its dust-corrected colour ($B - V$ or Gaia B_P–R_P) and the current rotation period alone.

Theoretical gyrochronology models need to consider many physical processes, initial rotation rates, properties of the magnetic field and stellar wind, or angular

momentum losses (e.g., Kawaler, 1988, 1989; Pinsonneault et al., 1989; van Saders and Pinsonneault, 2013; Matt et al., 2015; van Saders et al., 2016). On the other hand, empirical models (e.g., Barnes, 2003, 2007a; Mamajek and Hillenbrand, 2008; Angus et al., 2015, 2019a) are based on observations of rotation periods in clusters. In the era of space photometry surveys like TESS or K2, our knowledge of the rotation periods of members of stellar clusters has improved significantly, which causes the gyrochronology analyses based on observations and empirical relations to be widely used in literature. However, young clusters show a large scatter of observed rotation periods for stars of the same spectral type and old open clusters are rare. Hence, the empirical relations that reproduce relatively well data of one cluster have limiting applications on different clusters and field stars. They can, however, provide a reasonable estimate for the ages of a large variety of stars. Many authors continue updating and investigating rotation period distributions for large variety of clusters (e.g., Gruner and Barnes, 2020; Rebull et al., 2020; Curtis et al., 2020; Gordon et al., 2021). Currently, a wide range of ages is covered starting at a few Myr in star-forming regions (Rebull et al., 2004) through the Pleiades and Praesepe clusters (Hartman et al., 2010; Douglas et al., 2017) up to NGC 6774 with an age of ~ 2.5 Gyrs (Gruner and Barnes, 2020).

As described in Angus et al. (2019b), the gyrochronology relation used in the `stardate` code is derived based on the Praesepe cluster, fitting a broken power-law to observed rotation periods of stars from this cluster in the form:

$$logP_{rot} = c_a log(t) + \sum_{n=0}^{4} c_n [log(G_{Bp} - G_{Rp})]^n \,, \tag{1.1}$$

where t defines the age of a cluster. To study ages of field stars one can use such empirical relation, with coefficients derived on the Praesepe cluster, to compute curves for different ages and plot them together with the members of the well-defined clusters: Pleiades cluster (∼120 Myr; Hartman et al., 2010), M34 cluster (∼250 Myr; Meibom et al., 2011), M37 cluster (∼400 Myr; Hartman et al., 2009), M48 cluster (∼450 Myr; Barnes et al., 2015), Praesepe cluster (∼650 Myr; Douglas et al., 2017), NGC 6811 cluster (∼1 Gyr; Curtis et al., 2019), and NGC 6774 cluster (∼2.5 Gyr; Gruner and Barnes, 2020). It can be seen in Figure 1.7. We can split Figure 1.7 into three regions. The region of G-type and F-type stars with Gaia colour $G_{Bp} - G_{Rp}$ in the range $\sim 0.9 - 2.7$ which have a narrow range of rotation periods. These stars come to the MS with a wide range of rotation periods and spin down to a much narrower range. The break in distribution for Gaia colours $G_{Bp} - G_{Rp}$ smaller than ~ 0.9 with stars rotating much faster is the Kraft break (Kraft, 1967), where magnetic braking becomes less efficient for more massive stars. The general picture is that subsurface convective zones in stars with lower mass are responsible for a stellar wind which, in interaction with a magnetic field, slows down the stellar rotation rate. Finally, the break in distribution for M dwarfs with Gaia colours $G_{Bp} - G_{Rp}$ larger than ~ 2.7. Hence, we observe the bimodal distribution with early M dwarfs (on average slow rotators) and late M dwarfs (on average fast rotators). In the younger Pleiades cluster, such bimodal distribution is less obvious (Rebull et al., 2016). These properties are attributed to the balance between the spin-up of these stars by contraction and the angular momentum loss through the stellar wind. We can observe an increasing trend in rotation rate toward later spectral types because

the contraction of these stars is a relatively long process and is longer for late M dwarfs. As we show in later sections, by comparing a rotation period vs colour of studied stars to such a plot, we can obtain reasonable constraints about age. We can usually distinguish if the star is consistent, younger or older than the Praesepe cluster and, in specific cases, even more. Curtis et al. (2019) showed that for spectral types between G0 and F2, we can distinguish between the Praesepe (∼650 Myr) and NGC 6811 clusters (∼1 Gyr), while K dwarfs distributions overlap in both clusters. Agüeros et al. (2018) proposed that after stars reach the slow-rotating sequence by the age of Praesepe, they enter the temporary phase of reduced rotation braking, which is longer for stars with lower mass. Then older clusters, such as NGC 6774 (∼2.5 Gyr), appear to rotate slower despite the smaller number of members.

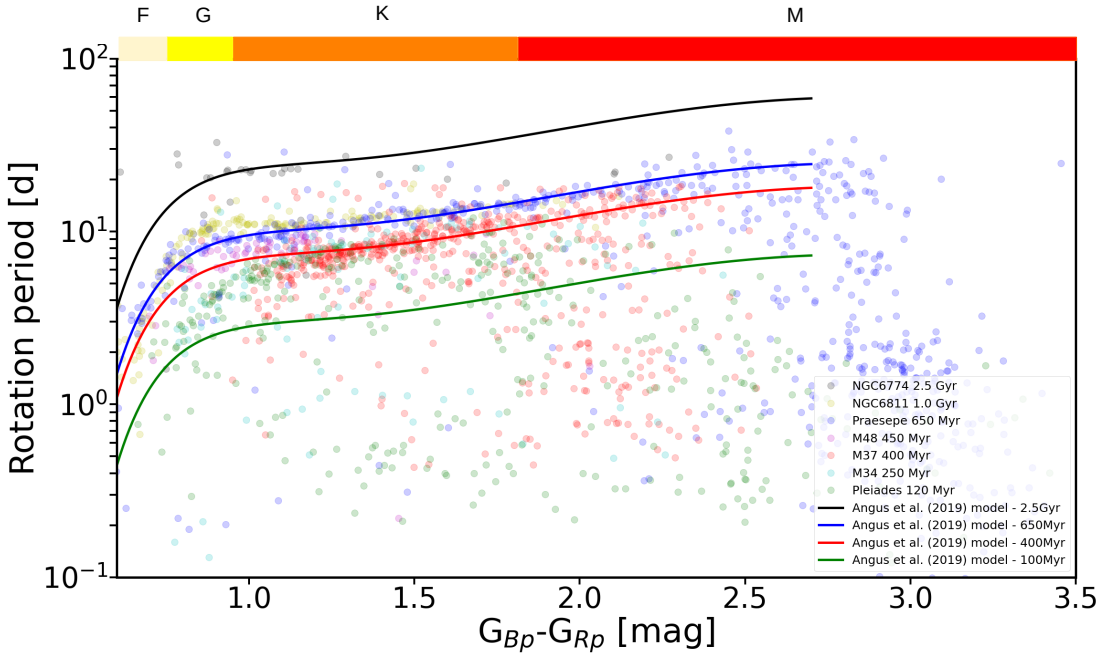

Figure 1.7: Color-period diagram of members of well-studied clusters: Pleiades cluster, M34 cluster, M37 cluster, M48 cluster, Praesepe cluster, NGC 6811 cluster, and NGC 6774 cluster. Lines represent the 100, 400, 650, and 2500 Myr curves computed from the empirical relation from Angus et al. (2019b).

Lithium equivalent width

Studies of the lithium equivalent width (EW) in stars in different clusters found a lithium dependency on the star's age and mass. Proton capture reactions are responsible for the destruction of lithium in the star's interior. The temperature needed for the reaction to occur is about 2.5 million Kelvins (e.g., Pinsonneault, 1997). Hence, lithium from the stellar atmosphere needs to be transported to the deeper and thus hotter layers of the star to be destroyed. In the pre-main-sequence phase, stars contract along fully-convective Hayashi tracks. Hence, the lithium burning triggered when cores reached the needed temperature. In stars with mass below 0.4 $M_\odot$, which remain fully convective, all lithium is early depleted. However, more massive stars develop a radiative core and stop mixing material

convectively to the core. Hence, lithium burning now depends on the temperature in the bottom part of the convective zone. In stars with mass below 0.6 $M_{\odot}$, such temperatures remain sufficient, and they burn all lithium. However, as in more massive stars the radiative core expands, the temperature in the bottom part of the convective zone will eventually drop below the needed temperature. In more massive stars, the radiative core develops before lithium burning is triggered; hence, they are expected to keep the initial lithium abundance.

These standard models of stellar evolution, which include convection as the only mixing mechanism (e.g., Soderblom et al., 1990), predict that stellar Li abundances should only be a function of effective temperature and age and that lithium depletion should not evolve after ~ 100 Myr. It is in contradiction with observations of stellar clusters of different ages and also with lithium observations of the Sun. Hence, additional mixing mechanisms in addition to convection were proposed that would mix material between the radiative core and the bottom part of the convective zone and hence also with a photosphere. These proposed mixing processes are rotational mixing, diffusion, mass loss or gravitational waves, in addition to convection (e.g., Duncan, 1981; Soderblom et al., 1995). Furthermore, observations indicate that lithium depletion also depends on a series of other factors, such as metallicity or magnetic activity (e.g., Deliyannis et al., 1990; Ventura et al., 1998; Jones et al., 1999; Charbonnel and Talon, 2005; Bouvier, 2008). All these are adding complications to the current models. Despite a lot of theoretical and observational effort, the available data revealed complex patterns that are not understood. Furthermore, it is important to note that the lithium content is expected to depend also on planetary companions; for instance, the planetary formation could change the initial angular momentum of the star, which, according to Takeda et al. (2010)) and Gonzalez et al. (2010), affect the process of lithium burning. Another alternative to an anomalous Li abundance is planet engulfment, which may lead to an increase in the Li abundance of a star (Montalbán and Rebolo, 2002; Sandquist et al., 2002).

Similarly, as with the rotation period, we can create the EW of Li vs. color plot of members of well-studied clusters (Figure 1.8): the Tuc-Hor young moving group (∼45 Myr; Mentuch et al., 2008), the Pleiades (∼120 Myr; Soderblom et al., 1993b), M34 (∼220 Myr; Jones et al., 1997), Ursa Major Group (∼400 Myr; Soderblom et al., 1993c), Praesepe (∼650 Myr; Soderblom et al., 1993a), Hyades (∼650 Myr; Soderblom et al., 1990), and M67 clusters (∼4 Gyr; Jones et al., 1999). The lithium line at 6708 Å can then be used to measure the lithium equivalent width of studied stars. Specifically, the EW corresponds to the area within the gaussian fit of the line. By comparing the Li EW vs colour of studied stars in such a plot, we can obtain some constraints about the age. We can see that usually, we can only distinguish between young and old stellar age. For $B - V$ colour larger than 0.75, we can distinguish younger age (based on the Pleiades and M34 clusters) from older age (based on the Praespe, Hyades and M 67 clusters) as stars from older clusters have lithium depleted. For smaller $B - V$ colours, we can also distinguish between these younger and older ages with some confidence level; however, only in specific cases when observations of Li EW lie far from the boundary.

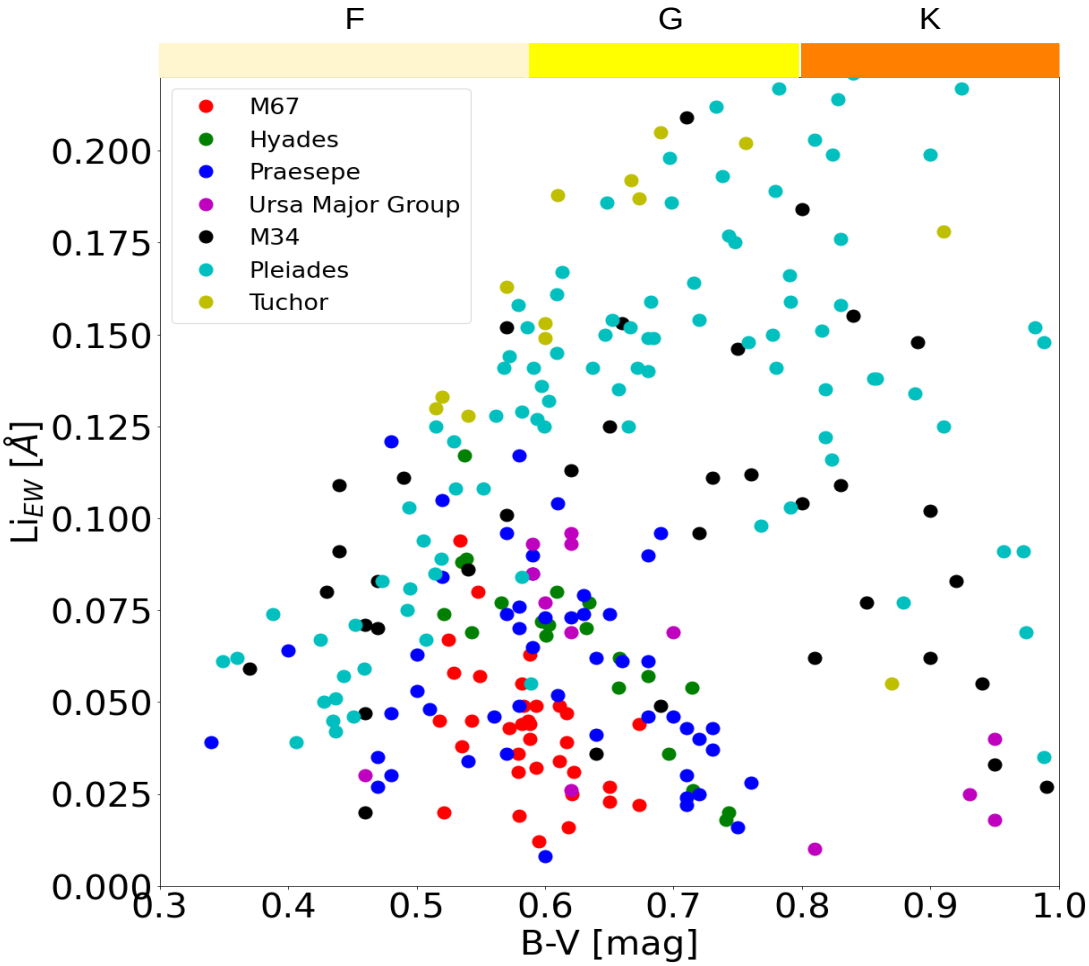

Figure 1.8: Colour vs EW of lithium line Li 6708 Å for members of well-studied clusters: Tuc-Hor young moving group, the Pleiades, M34, Ursa Major Group, Praesepe, Hyades, and M67 clusters.

X-ray luminosity

Firstly observed on the Sun, the stellar corona is a magnetically confined plasma with up to several million Kelvin temperatures. It is also the primary source of X-ray emission of a star. Corona heating is typically associated with the magnetic field or magnetic energy release, specifically (e.g., Erdélyi and Ballai, 2007). Such magnetic energy release, however, decreases with time as the rate of stellar rotation slows down. Spin down of stellar rotation is an observed property attributed to the angular momentum loss through the magnetically controlled stellar wind (e.g., Ivanova and Taam, 2003; Tout and Pringle, 1992). Ionized wind particles gain high specific angular momentum as they travel outward along spiral-shaped magnetic field lines that corotate with the star (Schatzman, 1962; Kawaler, 1988). Thus, corona heating becomes less and less efficient, and one would expect the X-ray emission to fall with a slowing rotation rate of stars. Indeed such a conclusion agrees with available observations, and the relation between activity/X-ray emission and rotation rate/age is intensively discussed (e.g., Pallavicini et al., 1981; Randich et al., 1996; Pizzolato et al., 2003). Furthermore, thanks to the available X-ray observations for a great number of stars from sur-

veys such as ROentgen SATellite (ROSAT; Voges et al., 1999), Chandra (Evans et al., 2010), or XMM–Newton telescopes (Jansen et al., 2001), we can also use X-ray luminosity as an age indicator comparing stars to well-studied clusters.

Similarly, as in the previous two sections, we can create the plot of the X-ray luminosity vs colour of members of well-studied clusters listed in Jackson et al. (2012) (see Figure 1.9) and compare these data with X-ray luminosities of studied stars to obtain some age constrains. The X-ray luminosity decay is slow for the first few hundred Myr, and we observe a scatter in luminosity in young clusters of at least one magnitude. The scatter is then smaller for the Praesepe and Hyades clusters. The main reason is the rotation-activity correlation (Noyes et al., 1984; Montalbán and Rebolo, 2002) and many stars in young clusters have different rotation rates before coming to the slow-rotating sequence. In terms of spectral type dependence, coronal activity decay follows the rotation rate changes. We discussed in the gyrochronology section that M stars spin down slowly, and hence for these stars, the X-ray luminosity is a poor age indicator even for older ages. As we show in later sections, by comparing an X-ray luminosity vs colour of studied stars to stellar clusters, we can usually use the Praesepe cluster to distinguish between young and old scenarios. Stars with an age of several Gyr are easily distinguishable as they typically have X-ray luminosity one magnitude or more below the stars from Praesepe.

R'$_{HK}$ index

A widely used age estimator for field stars is the R'$_{HK}$ index, which measures chromospheric emission in the cores of the Ca II H and K absorption lines, normalized to the underlying photospheric spectrum. Hence, it maps the chromospheric activity similarly to X-ray luminosity maps the coronal activity. Mamajek and Hillenbrand (2008) showed that fractional X-ray luminosity ($\log(L_X/L_{bol})$ and log R'$_{HK}$ are well correlated over a wide range of masses and ages for solar-type dwarfs. However, a very important advantage of the R'$_{HK}$ age indicator is that we have observational data for solar-like stars in the old M67 open cluster ($\sim$4 Gyr; Giampapa et al., 2006).

A decrease in chromosphere activity in time observed through the R'$_{HK}$ index can be used as an age indicator. Mamajek and Hillenbrand (2008) compiles data of R'$_{HK}$ index measurements for members of stellar associations from the literature to create empirical age-activity relations (see Figure 1.10). Based on these data, they derived the relation in the form:

$$log\tau = -38.053 - 17.912 log R'_{HK} - 1.6675 (log R'_{HK})^2, \tag{1.2}$$

where τ represents an age in years. The fit is only appropriate approximately between logR'$_{HK}$ values of -4.0 and -5.1 and logτ of 6.7 and 9.9 (the approximate range covered by cluster samples). We can see in Figure 1.10 that we can distinguish the age of several Gyr based on the M67 cluster ($\sim$4 Gyr). Then, we are not usually able to distinguish the Sco-Cen members ($\sim$5-15 Myr) from Pleiades ($\sim$120 Myr), but we are able to distinguish them from Hyades ($\sim$650 Myr). Finally, only in some specific locations (such as larger values of the R'$_{HK}$ index), we can distinguish Hyades from Pleiades.

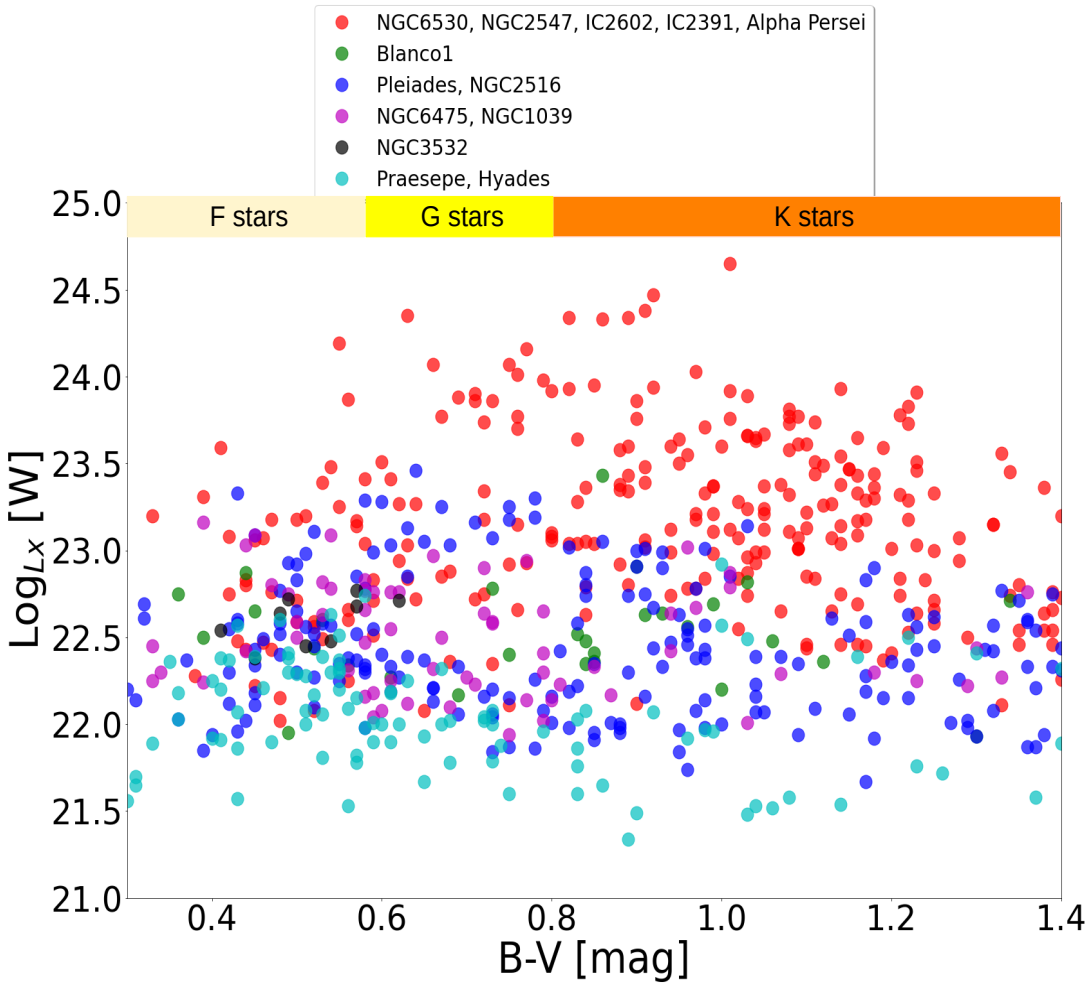

Figure 1.9: X-ray luminosity vs colour for members of well-defined clusters from Jackson et al. (2012).

Membership to young associations

Coeval young moving groups (YMGs) are formed from a single molecular cloud. In such a case, we can assume that all group members were formed in the same environment and share similar distances, ages and metallicities, hence applying collective parameters from these groups to each member. The members also share similar space velocities U, V, W. We can use kinematics information, such as proper motions, absolute radial velocities, and parallaxes for any star to determine their space velocities and to investigate their kinematic membership in YMGs. In recent years, Gaia (e.g., Gaia Collaboration et al., 2018, 2021) has significantly improved our knowledge on 3D spatial views of clusters and young moving groups (Gagné et al., 2018; Pang et al., 2021). While determining the age of field stars from age indicators is challenging, the membership would significantly improve the age precision (Bell et al., 2015). Various methods have been developed to identify members of young associations. In more complex algorithms, such as `BANYAN` (Gagné et al., 2018) and `LACEwING` (Riedel et al., 2017), associations are modelled with freely rotating tridimensional Gaussian ellipsoids in position and velocity spaces. Such ellipsoids taken from Gagné et al. (2018) can be seen in Figure 1.11. The regions shown in Figure 1.11 also correspond to stars in the

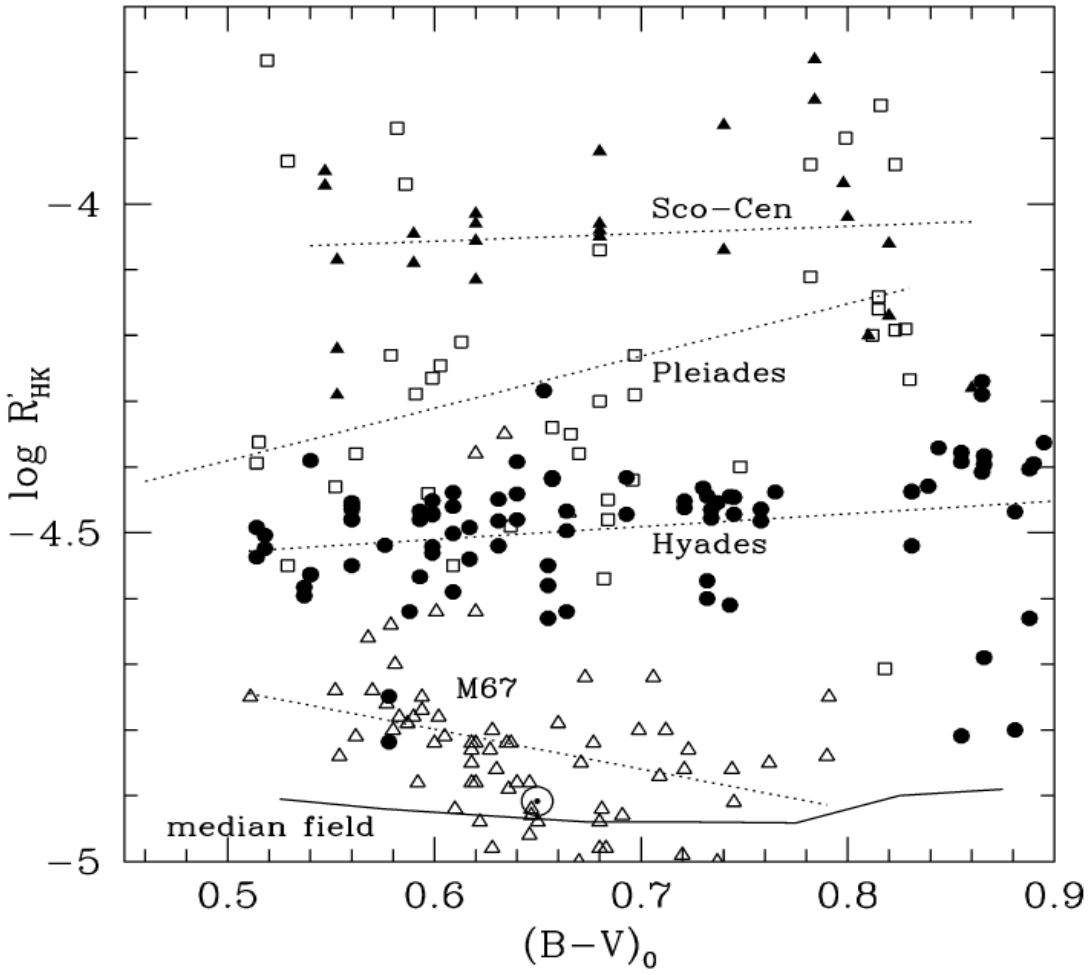

Figure 1.10: $B-V$ colour vs logR'$_{HK}$ for members of several well-studied stellar clusters from (Mamajek and Hillenbrand, 2008): Sco-Cen members, Pleiades, Hyades, and M67. Source: Mamajek and Hillenbrand (2008).

young disk (Leggett, 1992), which typically contains stars younger than 1 Gyr.

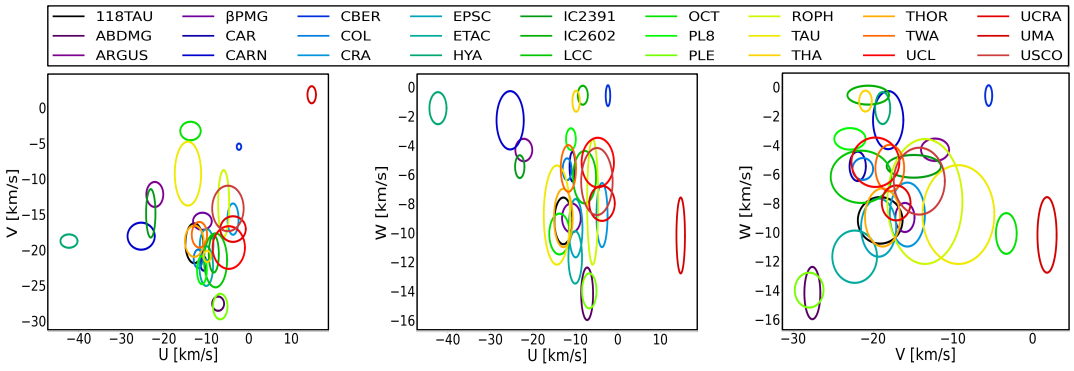

Figure 1.11: Membership to young associations. Ellipses represent the 1-sigma position of young stellar associations in space velocities U, V, W taken from Gagné et al. (2018).

2. Tidal interactions

This section presents a brief introduction to the theory of tidal interactions. It is partly based on my publication Šubjak et al. (2022).

Observations of orbital eccentricities of EGPs reveal a decreasing trend towards closer separations. It can be seen in Figure 2.1 where we plot the eccentricity vs orbital period of known exoplanets. Rasio and Ford (1996) proposed that tidal interactions between close EGPs and host stars may circularise the planet's orbits. As such interactions strongly depend on the orbital distance, it would explain the observed trend in the eccentricity distribution. Jackson et al. (2008) used the tidal evolution equations to predict the initial eccentricity distribution of close EGPs from the observed one using ages of EGPs from the literature. They found out that it matches the initial eccentricity distribution of the general population for relatively normal values of the stellar tidal quality factor. It may suggest that the difference between the initial and observed eccentricity distribution of close EGPs may be a result of tidal interactions.

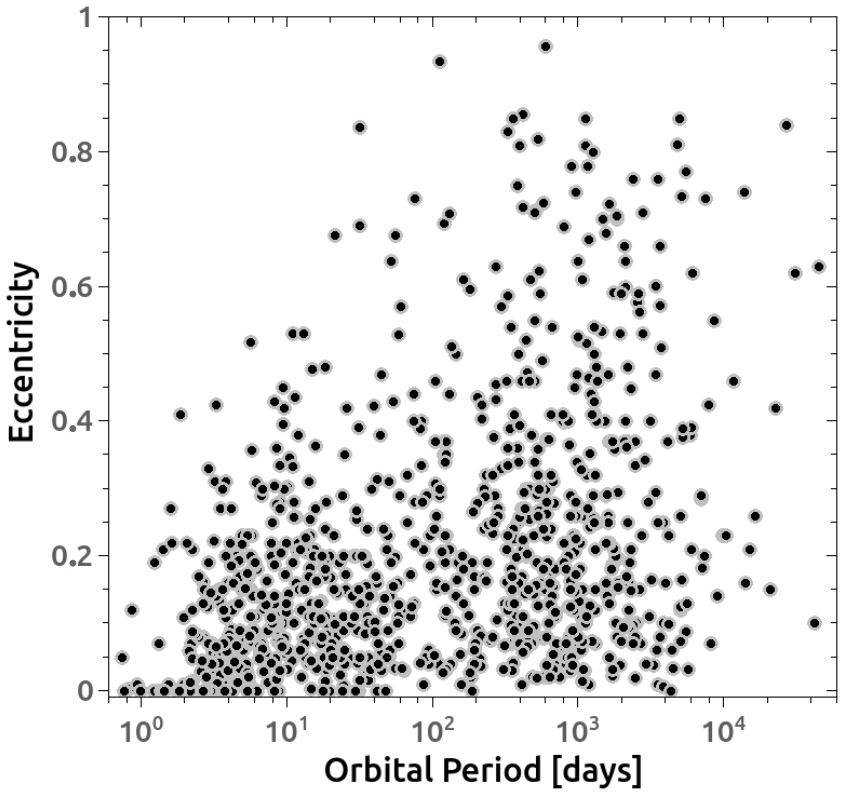

Figure 2.1: Eccentricity versus orbital period for the known planets characterised by radial velocity. Data from Fontanive and Bardalez Gagliuffi (2021).

There are several reasons why to study tidal interactions. First, the tidal evolution equations depend on the tidal quality factors of the SSO and the star. The tidal quality factors represent a parametrisation of the response of the body's interior to tidal perturbation and are quite difficult to determine theoretically. Observations of the tidal effect can constraints these factors. Second, there are

several interesting applications. If SSOs have eccentric orbits, we can derive lower limits for their masses as well as upper limits for their radii if we know one of these parameters. It is because the tidal circularisation timescale increases with the planet's radius and decreases with the planet's mass. Hence, we can obtain these limits by lowering radius or increasing mass to the point that the circularisation timescale is equal to the system age. However, here we assume that we already know the tidal quality factors. Third, if we observe an eccentric planet in an old system, where one would have expected the planet's orbit to be already circularised, we can suspect additional interactions from another planet or a distant companion. Finally, we expect that objects in the brown dwarf desert can form either at larger separations and then migrate or in-situ, close to the host star. It is crucial to measure the circularisation timescale (tidal quality factors together with stellar and planetary parameters) as precisely as possible to discuss how these objects form. As one particular example, we can use the transiting brown dwarf TOI-503b (Šubjak et al., 2020) with an age of ~ 180 Myr and zero eccentricity. If the circularisation timescale for this system is larger than its age, it would mean that the system formed at a very similar position and did not have time to migrate and circularise.

The tidal evolution equations were mathematically modelled by several authors (e.g., Jeffreys, 1961; Goldreich, 1963; MacDonald, 1964). Jackson et al. (2008) compiled useful equations rewritten to the form appropriate for close-in SSOs. According to them, the timescale for orbital circularisation for a close-in companion, τ_e, is:

$$\frac{1}{\tau_e} = \frac{\sqrt{GM_\star^3}}{M_\mathrm{p}} \left[\frac{63}{4} \frac{R_\mathrm{p}^5}{Q'_\mathrm{p}} + \frac{171}{16} \frac{R_\star^5}{Q'_\star} \left(\frac{M_\mathrm{p}}{M_\star} \right)^2 \right] a^{-\frac{13}{2}}, \tag{2.1}$$

where a is the semi-major axis, G is the gravitational constant, $Q'_\star$ and Q'_p are the tidal quality factors of the star and planet, respectively. The tidal dissipation parameters represent the ratio of the elastic energy stored to the energy dissipated per cycle of the tide – larger values of tidal factors lead to longer circularisation timescales. It is defined as:

$$Q^{-1} \equiv \frac{1}{2\pi E_0} \oint \left(- \frac{dE}{dt} \right) dt, \tag{2.2}$$

where E_0 is the peak energy stored in the tidal distortion during the cycle, dE/dt is the rate of dissipation and its integral defines the energy lost during the cycle (Goldreich and Soter, 1966). The tidal quality factor in Equation 2.1 further includes the Love number, the correction factor for the tidal-effective rigidity of the body and its radial density distribution, $Q' = 3Q/2k_2$ (Goldreich and Soter, 1966; Jackson et al., 2008). For an homogeneous fluid body $k_2 = 3/2$. The value of Q' is difficult to estimate, and possible values span large intervals from 10^2 for rocky planets (Clausen and Tilgner, 2015), to 10^{5-6} for some giant planets (Lainey et al., 2009), up to 10^{8-9} in case of some stars (Collier Cameron and Jardine, 2018), with typical scatter of several orders of magnitude.

The equation above has two components. The first depends on the tidal quality factor of the planet, and the second on the tidal quality factor of the star. Hence, the values of these factors, together with the planet's mass, will define which component is significant. The first component will always be dominant for

rocky planets. For giant planets, the first component is usually dominant, but the second component is also becoming important with increasing mass. For brown dwarfs, both components are important and with increasing mass, the second component becomes dominant. In binary stars, we are interested only in the second component. It means that while for planets, we are usually interested only in $Q'_{\rm p}$ in order to study tidal interactions, for brown dwarfs, we need to consider both $Q'_\star$ and $Q'_{\rm p}$, complicating the whole process. Another important thing to note is that the circularisation timescale in this form represents the exponential damping of eccentricity on this timescale; hence the time needed to circularise orbit fully is two or three times larger depending on the initial value of the eccentricity. Finally, in analyses of tidal interactions, we are comparing circularisation timescales with the ages of systems. It is justified by the assumption that the time the planet has spent at a small orbital distance is comparable with the age of the star. In other words, it is predicted that planets migrate inwards very early in the lifetimes of planetary systems (Trilling et al., 1998; Murray et al., 1998; Suárez Mascareño et al., 2021).

2.1 Stellar tidal quality factor

There is disagreement in the literature about the values of $Q'_\star$, with plausible values ranging from 10^5 to 10^8; furthermore, even for a single system, the value of $Q'_\star$ may change over time as the tidal forcing changes due to the orbital evolution of the system as well as stellar evolution (e.g., Jackson et al., 2008; Penev et al., 2012). Patel and Penev (2022) used the sample of 41 eclipsing binaries to restrict $Q'_\star$. They performed simulations of the rotation period evolution of these systems accounting for effects of tides, stellar evolution, and loss of stellar angular momentum via magnetic winds. They found that all stars in the sample (K–F type stars) can be relatively well described by $Q'_\star \sim 10^7$. Jackson et al. (2008) used the tidal evolution equations to model backwards the observed eccentricity distribution of close EGPs. They found that it matches the initial eccentricity distribution of the general population for $Q'_\star \sim 10^{5.5}$. Bonomo et al. (2017) used know eccentric EGPs at close orbits below 0.05 au to constrain $Q'_\star \sim 10^{6-7}$. Penev et al. (2018) modelled the tidal evolution in systems with hot Jupiters based on the rotation periods of host stars to find a dependence of $Q'_\star$ on the tidal forcing period and the range of possible values between $Q'_\star \sim 10^{5-7}$. The results of Collier Cameron and Jardine (2018) from the study of the tidal orbital decay of hot Jupiters suggest $Q'_\star \sim 10^8$.

2.2 Substellar tidal quality factor

There are only few brown dwarfs with published constraints on $Q'_{\rm BD}$ (Heller et al., 2010; Beatty et al., 2018). Heller et al. (2010) studied the tidal interactions in 2MASS J05352184-0546085 eclipsing brown dwarf binary. They used synchronisation timescales to restrict the tidal quality factor to $Q'_{\rm BD} \geq 4.5$. Beatty et al. (2018) studied the CWW 89 system with transiting BD on an eccentric orbit. They used the circularisation timescale to restrict the tidal quality factor to $Q'_{\rm BD} \geq 4.15$.

3. TOI-503: The first known brown dwarf-Am star binary from the TESS mission

This section presents the paper published in the Astronomical Journal about the discovery of the first transiting brown dwarf from the TESS space mission (Šubjak et al., 2020) (Attachment A). This section aims to derive the stellar and brown dwarf parameters as well as the orbital parameters of the system. Tidal interactions between the star and brown dwarf are then considered to discuss the formation history. Finally, the system is put into the context with the population of known transiting brown dwarfs.

4. TOI-1268b: The youngest hot Saturn-mass transiting exoplanet

This section presents the paper published in Astronomy & Astrophysics about the discovery of the youngest transiting Saturn-mass planet from the TESS space mission (Šubjak et al., 2022) (Attachment B). This section aims to derive the stellar and exoplanetary parameters as well as the orbital parameters of the system. The system parameters were then used to discuss tidal interactions and constrain the values of a tidal quality factor for non-inflated Saturn-mass planets. Finally, we discussed prospects for further atmospheric studies.

5. Search for planets around stars with wide brown dwarfs

This section presents the paper accepted for publication in Astronomy & Astrophysics about the population of planets in systems with a wide brown dwarf companion (Attachment C). We have spectroscopically followed up six bright stars with known wide brown dwarf companions to search for planets in these systems. This section aims to understand better the role of wide brown dwarf companions on planetary systems. Our approach search for possible peculiarities in parameter distributions of planets in systems with a wide BD companion, comparing them to distributions of the general planetary population.

Summary and outlook

In this thesis, I have presented discoveries of the first brown dwarf-Am star binary and the youngest Saturn-mass planet from the TESS space mission. Our goal was first to characterise these systems and then study tidal interactions between the companion and the host star. Tidal interactions provide a method to constrain the formation and evolution history, and with a larger sample of precisely characterised systems, we can expect a significant impact on the understanding of transiting SSOs in upcoming years. The tidal equations depend on the tidal quality factors, which are difficult to measure, and we found disagreement in the literature with a large range of possible values. Hence, we used the TOI-1268 system to investigate tidal interactions and put constraints on the tidal quality factor for Saturn-mass planets. We found an interval of possible values between $10^{4.5-5.3}$. It can be expanded for objects of all masses, and it demonstrates that with a large sample, we will be able to put robust constraints on these factors as well as discuss how the tidal quality factor behaves as the function of different parameters. It would help to better understand exoplanet interiors when merged with the theoretical studies. To assess the effect of the current uncertainties on the formation and evolution of SSOs, we used the TOI-503 system to derive the circularisation timescale as a function of the tidal quality factors. Because of its dependence on the tidal quality factors, this timescale can be either shorter or longer than the system age, meaning that we cannot explicitly say how the system formed. However, we provide preferred values for the tidal quality factor for the star and brown dwarf, which may indicate that the system formed in-situ. Furthermore, we also proposed that the brown dwarf can be linked with the Am phenomenon of the host star. Studies investigating Am stars revealed that about 60–70% of Am stars are binaries (Abt and Levy, 1985; Smalley et al., 2014; Carquillat and Prieur, 2007). However, all Am stars are slow rotators, and this slow rotation is attributed to the tidal interactions with the second component in a binary system. Hence, one would expect the binary ratio 100%. It implies that either (1) the binarity fraction is underestimated or (2) other mechanisms are needed to explain the nature of Am stars. Our idea is that SSOs around apparently single Am stars are filling this gap. Indeed, the previous studies were only sensitive to stellar companions. Additionally, several systems are known, with Am stars hosting a giant exoplanet in a close orbit (e.g., Siverd et al., 2018; Hellier et al., 2019; Addison et al., 2021). We plan to spectroscopically follow up several apparently single Am stars to search for SSOs in the future.

I have also presented results about the comparison of planetary parameter distributions between planets around single planet-host stars and planet-host stars with a wide stellar/substellar companion. Tidal interactions are studied through the system's observed properties; however, as many stars are part of multiple systems, to understand the formation and evolution of these systems, it is also important to understand interactions between wide companions and inner planets, which can cause peculiarities in their parameter distributions. Hence, we compiled systems with known planets from the literature and compared them with the sample of known planets with a wide stellar companion and planets in systems with a wide BD companion to search for possible peculiarities in their

parameter distributions. We observe an enhancement of planets with short periods below six days in systems with a wide stellar companion, which we interpret as a consequence of enhanced migration inwards closer to the host star. Such a trend was already mentioned in the literature. We also found that planets in systems with a wide BD companion follow their own eccentricity distribution with a maximum at ~ 0.65 and usually have periods larger than 40 days and masses larger than $0.1\,M_J$. Furthermore, we also observe a break at the eccentricity of 0.5 with a small number of planets with higher eccentricities in multi-planetary systems. So far, the sample is too small to make any firm conclusions. However, we may consider expanding this sample to reveal whether parameter distributions' peculiarities are significant.

Bibliography

T. M. C. Abbott, F. B. Abdalla, S. Allam, et al. The Dark Energy Survey: Data Release 1. *ApJS*, 239(2):18, December 2018. doi: 10.3847/1538-4365/aae9f0.

H. A. Abt and S. G. Levy. Improved study of metallic-line binaries. *ApJS*, 59: 229–247, October 1985. doi: 10.1086/191070.

Fred C. Adams and Marco Fatuzzo. A Theory of the Initial Mass Function for Star Formation in Molecular Clouds. *ApJ*, 464:256, June 1996. doi: 10.1086/177318.

Brett C. Addison, Emil Knudstrup, Ian Wong, et al. TOI-1431b/MASCARA-5b: A Highly Irradiated Ultrahot Jupiter Orbiting One of the Hottest and Brightest Known Exoplanet Host Stars. *AJ*, 162(6):292, December 2021. doi: 10.3847/1538-3881/ac224e.

Conny Aerts, Jørgen Christensen-Dalsgaard, and Donald W. Kurtz. *Asteroseismology*. 2010.

M. A. Agüeros, E. C. Bowsher, J. J. Bochanski, et al. A New Look at an Old Cluster: The Membership, Rotation, and Magnetic Activity of Low-mass Stars in the 1.3 Gyr Old Open Cluster NGC 752. *ApJ*, 862(1):33, July 2018. doi: 10.3847/1538-4357/aac6ed.

Mohamad Ali-Dib. Disentangling hot Jupiters formation location from their chemical composition. *MNRAS*, 467(3):2845–2854, May 2017. doi: 10.1093/mnras/stx260.

F. Allard, D. Homeier, and B. Freytag. Models of very-low-mass stars, brown dwarfs and exoplanets. *Philosophical Transactions of the Royal Society of London Series A*, 370(1968):2765–2777, June 2012. doi: 10.1098/rsta.2011.0269.

Ruth Angus, Suzanne Aigrain, Daniel Foreman-Mackey, et al. Calibrating gyrochronology using Kepler asteroseismic targets. *MNRAS*, 450(2):1787–1798, June 2015. doi: 10.1093/mnras/stv423.

Ruth Angus, Timothy Morton, and Daniel Foreman-Mackey. stardate: Combining dating methods for better stellar ages. *The Journal of Open Source Software*, 4(41):1469, September 2019a. doi: 10.21105/joss.01469.

Ruth Angus, Timothy D. Morton, Daniel Foreman-Mackey, et al. Toward Precise Stellar Ages: Combining Isochrone Fitting with Empirical Gyrochronology. *AJ*, 158(5):173, November 2019b. doi: 10.3847/1538-3881/ab3c53.

Martin Asplund, Nicolas Grevesse, A. Jacques Sauval, et al. The Chemical Composition of the Sun. *ARA&A*, 47(1):481–522, September 2009. doi: 10.1146/annurev.astro.46.060407.145222.

M. Auvergne, P. Bodin, L. Boisnard, et al. The CoRoT satellite in flight: description and performance. *A&A*, 506(1):411–424, October 2009. doi: 10.1051/0004-6361/200810860.

I. Baraffe, G. Chabrier, F. Allard, et al. Evolutionary models for low-mass stars and brown dwarfs: Uncertainties and limits at very young ages. *A&A*, 382: 563–572, February 2002. doi: 10.1051/0004-6361:20011638.

I. Baraffe, G. Chabrier, and T. Barman. The physical properties of extra-solar planets. *Reports on Progress in Physics*, 73(1):016901, January 2010. doi: 10.1088/0034-4885/73/1/016901.

R. J. Barber, J. Tennyson, G. J. Harris, et al. A high-accuracy computed water line list. *MNRAS*, 368(3):1087–1094, May 2006. doi: 10.1111/j.1365-2966.2006.10184.x.

Daniella C. Bardalez Gagliuffi, Adam J. Burgasser, Christopher R. Gelino, et al. SpeX Spectroscopy of Unresolved Very Low Mass Binaries. II. Identification of 14 Candidate Binaries with Late-M/Early-L and T Dwarf Components. *ApJ*, 794(2):143, October 2014. doi: 10.1088/0004-637X/794/2/143.

Sydney A. Barnes. On the Rotational Evolution of Solar- and Late-Type Stars, Its Magnetic Origins, and the Possibility of Stellar Gyrochronology. *ApJ*, 586 (1):464–479, March 2003. doi: 10.1086/367639.

Sydney A. Barnes. Ages for Illustrative Field Stars Using Gyrochronology: Viability, Limitations, and Errors. *ApJ*, 669(2):1167–1189, November 2007a. doi: 10.1086/519295.

Sydney A. Barnes. Ages for Illustrative Field Stars Using Gyrochronology: Viability, Limitations, and Errors. *ApJ*, 669(2):1167–1189, November 2007b. doi: 10.1086/519295.

Sydney A. Barnes, Joerg Weingrill, Thomas Granzer, et al. A color-period diagram for the open cluster M 48 (NGC 2548), and its rotational age. *A&A*, 583: A73, November 2015. doi: 10.1051/0004-6361/201526129.

Shantanu Basu and Eduard I. Vorobyov. A Hybrid Scenario for the Formation of Brown Dwarfs and Very Low Mass Stars. *ApJ*, 750(1):30, May 2012. doi: 10.1088/0004-637X/750/1/30.

A. Bayo, C. Rodrigo, D. Barrado Y Navascués, et al. VOSA: virtual observatory SED analyzer. An application to the Collinder 69 open cluster. *A&A*, 492(1): 277–287, December 2008. doi: 10.1051/0004-6361:200810395.

A. Bayo, D. Barrado, J. Stauffer, et al. Spectroscopy of very low mass stars and brown dwarfs in the Lambda Orionis star forming region. I. Enlarging the census down to the planetary mass domain in Collinder 69. *A&A*, 536:A63, December 2011. doi: 10.1051/0004-6361/201116617.

Thomas G. Beatty, Caroline V. Morley, Jason L. Curtis, et al. A Significant Overluminosity in the Transiting Brown Dwarf CWW 89Ab. *AJ*, 156(4):168, Oct 2018. doi: 10.3847/1538-3881/aad697.

Juliette C. Becker, Andrew Vanderburg, Fred C. Adams, et al. WASP-47: A Hot Jupiter System with Two Additional Planets Discovered by K2. *ApJ*, 812(2): L18, October 2015. doi: 10.1088/2041-8205/812/2/L18.

Cameron P. M. Bell, Eric E. Mamajek, and Tim Naylor. A self-consistent, absolute isochronal age scale for young moving groups in the solar neighbourhood. *MNRAS*, 454(1):593–614, November 2015. doi: 10.1093/mnras/stv1981.

D. H. Berger, D. R. Gies, H. A. McAlister, et al. First Results from the CHARA Array. IV. The Interferometric Radii of Low-Mass Stars. *ApJ*, 644(1):475–483, June 2006. doi: 10.1086/503318.

G. Bihain and R. D. Scholz. A non-uniform distribution of the nearest brown dwarfs. *A&A*, 589:A26, May 2016. doi: 10.1051/0004-6361/201528007.

Bertram Bitsch, Andre Izidoro, Anders Johansen, et al. Formation of planetary systems by pebble accretion and migration: growth of gas giants. *A&A*, 623: A88, March 2019. doi: 10.1051/0004-6361/201834489.

S. Blanco-Cuaresma, C. Soubiran, U. Heiter, et al. Determining stellar atmospheric parameters and chemical abundances of FGK stars with iSpec. *A&A*, 569:A111, September 2014. doi: 10.1051/0004-6361/201423945.

Sergi Blanco-Cuaresma. Modern stellar spectroscopy caveats. *MNRAS*, 486(2): 2075–2101, June 2019. doi: 10.1093/mnras/stz549.

P. Bodenheimer and J. B. Pollack. Calculations of the accretion and evolution of giant planets: The effects of solid cores. *Icarus*, 67(3):391–408, September 1986. doi: 10.1016/0019-1035(86)90122-3.

A. S. Bonomo, S. Desidera, S. Benatti, et al. The GAPS Programme with HARPS-N at TNG . XIV. Investigating giant planet migration history via improved eccentricity and mass determination for 231 transiting planets. *A&A*, 602:A107, June 2017. doi: 10.1051/0004-6361/201629882.

William J. Borucki, David Koch, Gibor Basri, et al. Kepler Planet-Detection Mission: Introduction and First Results. *Science*, 327(5968):977, February 2010. doi: 10.1126/science.1185402.

A. P. Boss. Gas Giant Protoplanets Formed by Disk Instability in Binary Star Systems. *ApJ*, 641(2):1148–1161, April 2006. doi: 10.1086/500530.

J. Bouvier. Lithium depletion and the rotational history of exoplanet host stars. *A&A*, 489(3):L53–L56, October 2008. doi: 10.1051/0004-6361:200810574.

Hervé Bouy, Wolfgang Brandner, Eduardo L. Martín, et al. Multiplicity of Nearby Free-Floating Ultracool Dwarfs: A Hubble Space Telescope WFPC2 Search for Companions. *AJ*, 126(3):1526–1554, September 2003. doi: 10.1086/377343.

Alessandro Bressan, Paola Marigo, Léo. Girardi, et al. PARSEC: stellar tracks and isochrones with the PAdova and TRieste Stellar Evolution Code. *MNRAS*, 427(1):127–145, November 2012. doi: 10.1111/j.1365-2966.2012.21948.x.

John M. Brewer, Debra A. Fischer, Sarbani Basu, et al. Accurate Gravities of F, G, and K stars from High Resolution Spectra Without External Constraints. *ApJ*, 805(2):126, June 2015. doi: 10.1088/0004-637X/805/2/126.

Timothy M. Brown and Ronald L. Gilliland. Asteroseismology. *ARA&A*, 32: 37–82, January 1994. doi: 10.1146/annurev.aa.32.090194.000345.

H. Bruntt, S. Basu, B. Smalley, et al. Accurate fundamental parameters and detailed abundance patterns from spectroscopy of 93 solar-type Kepler targets. *MNRAS*, 423(1):122–131, June 2012. doi: 10.1111/j.1365-2966.2012.20686.x.

Adam J. Burgasser, J. Davy Kirkpatrick, I. Neill Reid, et al. Binarity in Brown Dwarfs: T Dwarf Binaries Discovered with the Hubble Space Telescope Wide Field Planetary Camera 2. *ApJ*, 586(1):512–526, March 2003. doi: 10.1086/346263.

Adam J. Burgasser, Kelle L. Cruz, Michael Cushing, et al. SpeX Spectroscopy of Unresolved Very Low Mass Binaries. I. Identification of 17 Candidate Binaries Straddling the L Dwarf/T Dwarf Transition. *ApJ*, 710(2):1142–1169, February 2010. doi: 10.1088/0004-637X/710/2/1142.

Ben Burningham, D. J. Pinfield, P. W. Lucas, et al. 47 new T dwarfs from the UKIDSS Large Area Survey. *MNRAS*, 406(3):1885–1906, August 2010. doi: 10.1111/j.1365-2966.2010.16800.x.

Adam Burrows, W. B. Hubbard, J. I. Lunine, et al. The theory of brown dwarfs and extrasolar giant planets. *Reviews of Modern Physics*, 73(3):719–765, July 2001. doi: 10.1103/RevModPhys.73.719.

Caleb I. Cañas, Songhu Wang, Suvrath Mahadevan, et al. Kepler-730: A Hot Jupiter System with a Close-in, Transiting, Earth-sized Planet. *ApJ*, 870(2): L17, January 2019. doi: 10.3847/2041-8213/aafa1e.

E. Caffau, H. G. Ludwig, M. Steffen, et al. Solar Chemical Abundances Determined with a CO5BOLD 3D Model Atmosphere. *Sol. Phys.*, 268(2):255–269, February 2011. doi: 10.1007/s11207-010-9541-4.

P. A. Cargile, D. J. James, and R. D. Jeffries. Identification of the Lithium Depletion Boundary and Age of the Southern Open Cluster Blanco 1. *ApJ*, 725(2):L111–L116, December 2010. doi: 10.1088/2041-8205/725/2/L111.

P. A. Cargile, D. J. James, J. Pepper, et al. Evaluating Gyrochronology on the Zero-age-main-sequence: Rotation Periods in the Southern Open Cluster Blanco 1 from the KELT-South Survey. *ApJ*, 782(1):29, February 2014. doi: 10.1088/0004-637X/782/1/29.

Theron W. Carmichael, Samuel N. Quinn, Alexander J. Mustill, et al. Two Intermediate-mass Transiting Brown Dwarfs from the TESS Mission. *AJ*, 160 (1):53, July 2020. doi: 10.3847/1538-3881/ab9b84.

Theron W. Carmichael, Samuel N. Quinn, George Zhou, et al. TOI-811b and TOI-852b: New Transiting Brown Dwarfs with Similar Masses and Very Different Radii and Ages from the TESS Mission. *AJ*, 161(2):97, February 2021. doi: 10.3847/1538-3881/abd4e1.

A. Carnero Rosell, B. Santiago, M. dal Ponte, et al. Brown dwarf census with the Dark Energy Survey year 3 data and the thin disc scale height of early L types. *MNRAS*, 489(4):5301–5325, November 2019. doi: 10.1093/mnras/stz2398.

J. M. Carquillat and J. L. Prieur. Contribution to the search for binaries among Am stars - VIII. New spectroscopic orbits of eight systems and statistical study of a sample of 91 Am stars. *MNRAS*, 380(3):1064–1078, September 2007. doi: 10.1111/j.1365-2966.2007.12143.x.

R. Cayrel, C. van't Veer-Menneret, N. F. Allard, and C. Stehlé. The Hα Balmer line as an effective temperature criterion. I. Calibration using 1D model stellar atmospheres. *A&A*, 531:A83, July 2011. doi: 10.1051/0004-6361/201116911.

G. Chabrier, A. Johansen, M. Janson, et al. Giant Planet and Brown Dwarf Formation. In Henrik Beuther, Ralf S. Klessen, Cornelis P. Dullemond, and Thomas Henning, editors, *Protostars and Planets VI*, page 619, January 2014. doi: 10.2458/azu_uapress_9780816531240-ch027.

Gilles Chabrier. Galactic Stellar and Substellar Initial Mass Function. *PASP*, 115(809):763–795, July 2003. doi: 10.1086/376392.

K. C. Chambers, E. A. Magnier, N. Metcalfe, et al. The Pan-STARRS1 Surveys. *arXiv e-prints*, art. arXiv:1612.05560, December 2016.

Corinne Charbonnel and Suzanne Talon. Influence of Gravity Waves on the Internal Rotation and Li Abundance of Solar-Type Stars. *Science*, 309(5744): 2189–2191, September 2005. doi: 10.1126/science.1116849.

Sourav Chatterjee, Eric B. Ford, Soko Matsumura, et al. Dynamical Outcomes of Planet-Planet Scattering. *ApJ*, 686(1):580–602, October 2008. doi: 10.1086/590227.

A. Chiavassa, L. Casagrande, R. Collet, et al. The STAGGER-grid: A grid of 3D stellar atmosphere models. V. Synthetic stellar spectra and broad-band photometry. *A&A*, 611:A11, March 2018. doi: 10.1051/0004-6361/201732147.

Jieun Choi, Aaron Dotter, Charlie Conroy, et al. Mesa Isochrones and Stellar Tracks (MIST). I. Solar-scaled Models. *ApJ*, 823(2):102, June 2016. doi: 10.3847/0004-637X/823/2/102.

Jørgen Christensen-Dalsgaard. Physics of solar-like oscillations. *Sol. Phys.*, 220 (2):137–168, April 2004. doi: 10.1023/B:SOLA.0000031392.43227.7d.

N. Clausen and A. Tilgner. Dissipation in rocky planets for strong tidal forcing. *A&A*, 584:A60, December 2015. doi: 10.1051/0004-6361/201526082.

P. R. T. Coelho. A new library of theoretical stellar spectra with scaled-solar and α-enhanced mixtures. *MNRAS*, 440(2):1027–1043, May 2014. doi: 10.1093/mnras/stu365.

Gavin A. L. Coleman, John C. B. Papaloizou, and Richard P. Nelson. In situ accretion of gaseous envelopes on to planetary cores embedded in evolving protoplanetary discs. *MNRAS*, 470(3):3206–3219, September 2017. doi: 10.1093/mnras/stx1297.

Andrew Collier Cameron and Moira Jardine. Hierarchical Bayesian calibration of tidal orbit decay rates among hot Jupiters. *MNRAS*, 476(2):2542–2555, May 2018. doi: 10.1093/mnras/sty292.

Jason Lee Curtis, Marcel A. Agüeros, Stephanie T. Douglas, et al. A Temporary Epoch of Stalled Spin-down for Low-mass Stars: Insights from NGC 6811 with Gaia and Kepler. *ApJ*, 879(1):49, July 2019. doi: 10.3847/1538-4357/ab2393.

Jason Lee Curtis, Marcel A. Agüeros, Sean P. Matt, et al. *ApJ*, 904(2):140, December 2020. doi: 10.3847/1538-4357/abbf58.

Michael C. Cushing, J. Davy Kirkpatrick, Christopher R. Gelino, et al. The Discovery of Y Dwarfs using Data from the Wide-field Infrared Survey Explorer (WISE). *ApJ*, 743(1):50, December 2011. doi: 10.1088/0004-637X/743/1/50.

R. M. Cutri, M. F. Skrutskie, S. van Dyk, et al. VizieR Online Data Catalog: 2MASS All-Sky Catalog of Point Sources (Cutri+ 2003). *VizieR Online Data Catalog*, art. II/246, June 2003.

R. M. Cutri, E. L. Wright, T. Conrow, et al. VizieR Online Data Catalog: AllWISE Data Release (Cutri+ 2013). *VizieR Online Data Catalog*, art. II/328, February 2021.

C. Damiani and R. F. Díaz. Can brown dwarfs survive on close orbits around convective stars? *A&A*, 589:A55, May 2016. doi: 10.1051/0004-6361/201527100.

Niall R. Deacon, Michael C. Liu, Eugene A. Magnier, et al. Four New T Dwarfs Identified in Pan-STARRS 1 Commissioning Data. *AJ*, 142(3):77, September 2011. doi: 10.1088/0004-6256/142/3/77.

Niall R. Deacon, Michael C. Liu, Eugene A. Magnier, et al. Wide Cool and Ultracool Companions to Nearby Stars from Pan-STARRS 1. *ApJ*, 792(2):119, September 2014. doi: 10.1088/0004-637X/792/2/119.

Constantine P. Deliyannis, Pierre Demarque, and Steven D. Kawaler. Lithium in Halo Stars from Standard Stellar Evolution. *ApJS*, 73:21, May 1990. doi: 10.1086/191439.

S. Desidera and M. Barbieri. Properties of planets in binary systems. The role of binary separation. *A&A*, 462(1):345–353, January 2007. doi: 10.1051/0004-6361:20066319.

R. F. Díaz, G. Montagnier, J. Leconte, et al. SOPHIE velocimetry of Kepler transit candidates. XIII. KOI-189 b and KOI-686 b: two very low-mass stars in long-period orbits. *A&A*, 572:A109, December 2014. doi: 10.1051/0004-6361/201424406.

Aaron Dotter, Brian Chaboyer, Darko Jevremović, Veselin Kostov, E. Baron, and Jason W. Ferguson. The Dartmouth Stellar Evolution Database. *ApJS*, 178 (1):89–101, September 2008. doi: 10.1086/589654.

S. T. Douglas, M. A. Agüeros, K. R. Covey, et al. Poking the Beehive from Space: K2 Rotation Periods for Praesepe. *ApJ*, 842(2):83, June 2017. doi: 10.3847/1538-4357/aa6e52.

G. Duchêne. Binary fraction in low-mass star forming regions: a reexamination of the possible excesses and implications. *A&A*, 341:547–552, January 1999.

D. K. Duncan. Lithium abundances, K line emission and ages of nearby solar type stars. *ApJ*, 248:651–669, September 1981. doi: 10.1086/159190.

A. Eggenberger, S. Udry, and M. Mayor. Statistical properties of exoplanets. III. Planet properties and stellar multiplicity. *A&A*, 417:353–360, April 2004. doi: 10.1051/0004-6361:20034164.

N. Epchtein, B. de Batz, L. Capoani, et al. The deep near-infrared southern sky survey (DENIS). *The Messenger*, 87:27–34, March 1997.

Courtney R. Epstein and Marc H. Pinsonneault. How Good a Clock is Rotation? The Stellar Rotation-Mass-Age Relationship for Old Field Stars. *ApJ*, 780(2): 159, January 2014. doi: 10.1088/0004-637X/780/2/159.

R. Erdélyi and I. Ballai. Heating of the solar and stellar coronae: a review. *Astronomische Nachrichten*, 328(8):726–733, October 2007. doi: 10.1002/asna.200710803.

Ian N. Evans, Francis A. Primini, Kenny J. Glotfelty, et al. The Chandra Source Catalog. *ApJS*, 189(1):37–82, July 2010. doi: 10.1088/0067-0049/189/1/37.

Jacqueline K. Faherty, Adam J. Burgasser, Andrew A. West, et al. The Brown Dwarf Kinematics Project. II. Details on Nine Wide Common Proper Motion Very Low Mass Companions to Nearby Stars. *AJ*, 139(1):176–194, January 2010. doi: 10.1088/0004-6256/139/1/176.

Debra A. Fischer and Jeff Valenti. The Planet-Metallicity Correlation. *ApJ*, 622 (2):1102–1117, April 2005. doi: 10.1086/428383.

M. J. Fogg and R. P. Nelson. Oligarchic and giant impact growth of terrestrial planets in the presence of gas giant planet migration. *A&A*, 441(2):791–806, October 2005. doi: 10.1051/0004-6361:20053453.

M. J. Fogg and R. P. Nelson. On the formation of terrestrial planets in hot-Jupiter systems. *A&A*, 461(3):1195–1208, January 2007. doi: 10.1051/0004-6361:20066171.

Clémence Fontanive and Daniella Bardalez Gagliuffi. The Census of Exoplanets in Visual Binaries: population trends from a volume-limited Gaia DR2 and literature search. *Frontiers in Astronomy and Space Sciences*, 8:16, March 2021. doi: 10.3389/fspas.2021.625250.

Malcolm Fridlund, Eric Gaidos, Oscar Barragán, et al. K2-111 b - a short period super-Earth transiting a metal poor, evolved old star. *A&A*, 604:A16, July 2017. doi: 10.1051/0004-6361/201730822.

Jonathan Gagné, Eric E. Mamajek, Lison Malo, et al. BANYAN. XI. The BANYAN Σ Multivariate Bayesian Algorithm to Identify Members of Young Associations with 150 pc. *ApJ*, 856(1):23, March 2018. doi: 10.3847/1538-4357/aaae09.

Gaia Collaboration, A. G. A. Brown, A. Vallenari, et al. Gaia Data Release 2. Summary of the contents and survey properties. *A&A*, 616:A1, August 2018. doi: 10.1051/0004-6361/201833051.

Gaia Collaboration, A. G. A. Brown, A. Vallenari, et al. Gaia Early Data Release 3. Summary of the contents and survey properties. *A&A*, 649:A1, May 2021. doi: 10.1051/0004-6361/202039657.

F. Gallet and J. Bouvier. Improved angular momentum evolution model for solar-like stars. II. Exploring the mass dependence. *A&A*, 577:A98, May 2015. doi: 10.1051/0004-6361/201525660.

Luan Ghezzi, Benjamin T. Montet, and John Asher Johnson. Retired A Stars Revisited: An Updated Giant Planet Occurrence Rate as a Function of Stellar Metallicity and Mass. *ApJ*, 860(2):109, June 2018. doi: 10.3847/1538-4357/aac37c.

Mark S. Giampapa, Jeffrey C. Hall, Richard R. Radick, et al. A Survey of Chromospheric Activity in the Solar-Type Stars in the Open Cluster M67. *ApJ*, 651(1):444–461, November 2006. doi: 10.1086/507624.

Ronald L. Gilliland, Timothy M. Brown, Jørgen Christensen-Dalsgaard, et al. Kepler Asteroseismology Program: Introduction and First Results. *PASP*, 122 (888):131, February 2010. doi: 10.1086/650399.

P. Goldreich. On the eccentricity of satellite orbits in the solar system. *MNRAS*, 126:257, January 1963. doi: 10.1093/mnras/126.3.257.

Peter Goldreich and Steven Soter. Q in the Solar System. *Icarus*, 5(1):375–389, January 1966. doi: 10.1016/0019-1035(66)90051-0.

G. Gonzalez, M. K. Carlson, and R. W. Tobin. Parent stars of extrasolar planets - X. Lithium abundances and v sini revisited. *MNRAS*, 403(3):1368–1380, April 2010. doi: 10.1111/j.1365-2966.2009.16195.x.

S. P. Goodwin and P. Kroupa. Limits on the primordial stellar multiplicity. *A&A*, 439(2):565–569, August 2005. doi: 10.1051/0004-6361:20052654.

Tyler A. Gordon, James R. A. Davenport, Ruth Angus, et al. Stellar Rotation in the K2 Sample: Evidence for Modified Spin-down. *ApJ*, 913(1):70, May 2021. doi: 10.3847/1538-4357/abf63e.

Richard O. Gray. SPECTRUM: A stellar spectral synthesis program. Astrophysics Source Code Library, record ascl:9910.002, October 1999.

D. Grether and C. H. Lineweaver. How Dry is the Brown Dwarf Desert? Quantifying the Relative Number of Planets, Brown Dwarfs, and Stellar Companions around Nearby Sun-like Stars. *ApJ*, 640:1051–1062, April 2006. doi: 10.1086/500161.

N. Grevesse, A. Noels, and A. J. Sauval. A revision of the solar abundance of dysprosium. *A&A*, 271:587, April 1993.

D. Gruner and S. A. Barnes. Rotation periods for cool stars in the open cluster Ruprecht 147 (NGC 6774). Implications for gyrochronology. *A&A*, 644:A16, December 2020. doi: 10.1051/0004-6361/202038984.

B. Gustafsson, B. Edvardsson, K. Eriksson, et al. A grid of MARCS model atmospheres for late-type stars. I. Methods and general properties. *A&A*, 486 (3):951–970, August 2008. doi: 10.1051/0004-6361:200809724.

J. D. Hartman, B. S. Gaudi, M. H. Pinsonneault, et al. Deep MMT Transit Survey of the Open Cluster M37. III. Stellar Rotation at 550 Myr. *ApJ*, 691 (1):342–364, January 2009. doi: 10.1088/0004-637X/691/1/342.

J. D. Hartman, G. Á. Bakos, G. Kovács, et al. A large sample of photometric rotation periods for FGK Pleiades stars. *MNRAS*, 408(1):475–489, October 2010. doi: 10.1111/j.1365-2966.2010.17147.x.

Artie P. Hatzes and Heike Rauer. A Definition for Giant Planets Based on the Mass-Density Relationship. *ApJ*, 810(2):L25, September 2015. doi: 10.1088/2041-8205/810/2/L25.

Suzanne L. Hawley, Kevin R. Covey, Gillian R. Knapp, et al. Characterization of M, L, and T Dwarfs in the Sloan Digital Sky Survey. *AJ*, 123(6):3409–3427, June 2002. doi: 10.1086/340697.

U. Heiter, K. Lind, M. Asplund, et al. Atomic and molecular data for optical stellar spectroscopy. *Phys. Scr*, 90(5):054010, May 2015. doi: 10.1088/0031-8949/90/5/054010.

R. Heller, B. Jackson, R. Barnes, et al. Tidal effects on brown dwarfs: application to the eclipsing binary 2MASS J05352184-0546085. The anomalous temperature reversal in the context of tidal heating. *A&A*, 514:A22, May 2010. doi: 10.1051/0004-6361/200912826.

Coel Hellier, D. R. Anderson, K. Barkaoui, et al. WASP-South hot Jupiters: WASP-178b, WASP-184b, WASP-185b, and WASP-192b. *MNRAS*, 490(1):1479–1487, November 2019. doi: 10.1093/mnras/stz2713.

Patrick Hennebelle. The FRIGG project: From intermediate galactic scales to self-gravitating cores. *A&A*, 611:A24, March 2018. doi: 10.1051/0004-6361/201731071.

Patrick Hennebelle and Gilles Chabrier. Analytical Theory for the Initial Mass Function: CO Clumps and Prestellar Cores. *ApJ*, 684(1):395–410, September 2008. doi: 10.1086/589916.

E. Høg, C. Fabricius, V. V. Makarov, et al. Construction and verification of the Tycho-2 Catalogue. *A&A*, 357:367–386, May 2000.

Chelsea X. Huang, Samuel N. Quinn, Andrew Vanderburg, et al. TESS Spots a Hot Jupiter with an Inner Transiting Neptune. *ApJ*, 892(1):L7, March 2020. doi: 10.3847/2041-8213/ab7302.

Daniel Huber, William J. Chaplin, Jørgen Christensen-Dalsgaard, et al. Fundamental Properties of Kepler Planet-candidate Host Stars using Asteroseismology. *ApJ*, 767(2):127, April 2013. doi: 10.1088/0004-637X/767/2/127.

Jonathan Irwin and Jerome Bouvier. The rotational evolution of low-mass stars. In Eric E. Mamajek, David R. Soderblom, and Rosemary F. G. Wyse, editors, *The Ages of Stars*, volume 258, pages 363–374, June 2009. doi: 10.1017/S1743921309032025.

D. Ishihara, T. Onaka, H. Kataza, et al. The AKARI/IRC mid-infrared all-sky survey. *A&A*, 514:A1, May 2010. doi: 10.1051/0004-6361/200913811.

N. Ivanova and Ronald E. Taam. Magnetic Braking Revisited. *ApJ*, 599(1): 516–521, December 2003. doi: 10.1086/379192.

Alan P. Jackson, Timothy A. Davis, and Peter J. Wheatley. The coronal X-ray-age relation and its implications for the evaporation of exoplanets. *MNRAS*, 422(3):2024–2043, May 2012. doi: 10.1111/j.1365-2966.2012.20657.x.

Brian Jackson, Richard Greenberg, and Rory Barnes. Tidal Evolution of Close-in Extrasolar Planets. *ApJ*, 678(2):1396–1406, May 2008. doi: 10.1086/529187.

F. Jansen, D. Lumb, B. Altieri, et al. XMM-Newton observatory. I. The spacecraft and operations. *A&A*, 365:L1–L6, January 2001. doi: 10.1051/0004-6361:20000036.

H. Jeffreys. The effect of tidal friction on eccentricity and inclination. *MNRAS*, 122:339–343, January 1961. doi: 10.1093/mnras/122.4.339.

Anders Johansen and Michiel Lambrechts. Forming Planets via Pebble Accretion. *Annual Review of Earth and Planetary Sciences*, 45(1):359–387, August 2017. doi: 10.1146/annurev-earth-063016-020226.

John Asher Johnson, R. Paul Butler, Geoffrey W. Marcy, et al. A New Planet around an M Dwarf: Revealing a Correlation between Exoplanets and Stellar Mass. *ApJ*, 670(1):833–840, November 2007. doi: 10.1086/521720.

John Asher Johnson, Kimberly M. Aller, Andrew W. Howard, et al. Giant Planet Occurrence in the Stellar Mass-Metallicity Plane. *PASP*, 122(894):905, August 2010. doi: 10.1086/655775.

Burton F. Jones, Debra Fischer, Matthew Shetrone, et al. The Evolution of the Lithium Abundances of Solar-Type Stars.VII.M34 (NGC 1039) and the Role of Rotation in Lithium Depletion. *AJ*, 114:352–362, July 1997. doi: 10.1086/118479.

Burton F. Jones, Debra Fischer, and David R. Soderblom. The Evolution of the Lithium Abundances of Solar-Type Stars. VIII. M67 (NGC 2682). *AJ*, 117(1): 330–338, January 1999. doi: 10.1086/300664.

Mario Jurić and Scott Tremaine. Dynamical Origin of Extrasolar Planet Eccentricity Distribution. *ApJ*, 686(1):603–620, October 2008. doi: 10.1086/590047.

Steven D. Kawaler. Angular Momentum Loss in Low-Mass Stars. *ApJ*, 333:236, October 1988. doi: 10.1086/166740.

Steven D. Kawaler. Rotational Dating of Middle-aged Stars. *ApJ*, 343:L65, August 1989. doi: 10.1086/185512.

Aurora Y. Kesseli, Andrew A. West, Mark Veyette, et al. An Empirical Template Library of Stellar Spectra for a Wide Range of Spectral Classes, Luminosity Classes, and Metallicities Using SDSS BOSS Spectra. *ApJS*, 230(2):16, June 2017. doi: 10.3847/1538-4365/aa656d.

J. Davy Kirkpatrick, Michael C. Cushing, Christopher R. Gelino, et al. The First Hundred Brown Dwarfs Discovered by the Wide-field Infrared Survey Explorer (WISE). *ApJS*, 197(2):19, December 2011. doi: 10.1088/0067-0049/197/2/19.

J. Davy Kirkpatrick, Christopher R. Gelino, Jacqueline K. Faherty, et al. The Field Substellar Mass Function Based on the Full-sky 20 pc Census of 525 L, T, and Y Dwarfs. *ApJS*, 253(1):7, March 2021. doi: 10.3847/1538-4365/abd107.

Robert P. Kraft. Studies of Stellar Rotation. V. The Dependence of Rotation on Age among Solar-Type Stars. *ApJ*, 150:551, November 1967. doi: 10.1086/149359.

Robert L. Kurucz. *SYNTHE spectrum synthesis programs and line data*. 1993.

David Lafrenière, Ray Jayawardhana, Alexis Brandeker, et al. A Multiplicity Census of Young Stars in Chamaeleon I. *ApJ*, 683(2):844–861, August 2008. doi: 10.1086/590239.

Valéry Lainey, Jean-Eudes Arlot, Özgür Karatekin, et al. Strong tidal dissipation in Io and Jupiter from astrometric observations. *Nature*, 459(7249):957–959, June 2009. doi: 10.1038/nature08108.

A. Lawrence, S. J. Warren, O. Almaini, et al. The UKIRT Infrared Deep Sky Survey (UKIDSS). *MNRAS*, 379(4):1599–1617, August 2007. doi: 10.1111/j.1365-2966.2007.12040.x.

S. K. Leggett. Infrared Colors of Low-Mass Stars. *ApJS*, 82:351, September 1992. doi: 10.1086/191720.

T. Lejeune and D. Schaerer. Database of Geneva stellar evolution tracks and isochrones for $(UBV)_J(RI)_C$ JHKLL'M, HST-WFPC2, Geneva and Washington photometric systems. *A&A*, 366:538–546, February 2001. doi: 10.1051/0004-6361:20000214.

Joanna L. Levine, Aaron Steinhauer, Richard J. Elston, et al. Low-Mass Stars and Brown Dwarfs in NGC 2024: Constraints on the Substellar Mass Function. *ApJ*, 646(2):1215–1229, August 2006. doi: 10.1086/504964.

Michael R. Line, Matteo Brogi, Jacob L. Bean, et al. A solar C/O and sub-solar metallicity in a hot Jupiter atmosphere. *Nature*, 598(7882):580–584, October 2021. doi: 10.1038/s41586-021-03912-6.

N. Lodieu, D. J. Pinfield, S. K. Leggett, et al. Eight new T4.5-T7.5 dwarfs discovered in the UKIDSS Large Area Survey Data Release 1. *MNRAS*, 379 (4):1423–1430, August 2007. doi: 10.1111/j.1365-2966.2007.12023.x.

N. Lodieu, B. Burningham, A. Day-Jones, et al. First T dwarfs in the VISTA Hemisphere Survey. *A&A*, 548:A53, December 2012. doi: 10.1051/0004-6361/201220182.

K. L. Luhman. New Brown Dwarfs and an Updated Initial Mass Function in Taurus. *ApJ*, 617(2):1216–1232, December 2004. doi: 10.1086/425647.

K. L. Luhman. The Stellar Population of the Chamaeleon I Star-forming Region. *ApJS*, 173(1):104–136, November 2007. doi: 10.1086/520114.

Gordon J. F. MacDonald. Tidal Friction. *Reviews of Geophysics and Space Physics*, 2:467–541, January 1964. doi: 10.1029/RG002i003p00467.

Nikku Madhusudhan, Joseph Harrington, Kevin B. Stevenson, et al. A high C/O ratio and weak thermal inversion in the atmosphere of exoplanet WASP-12b. *Nature*, 469(7328):64–67, January 2011. doi: 10.1038/nature09602.

Eric E. Mamajek and Lynne A. Hillenbrand. Improved Age Estimation for Solar-Type Dwarfs Using Activity-Rotation Diagnostics. *ApJ*, 687(2):1264–1293, November 2008. doi: 10.1086/591785.

Avi M. Mandell, Sean N. Raymond, and Steinn Sigurdsson. Formation of Earth-like Planets During and After Giant Planet Migration. *ApJ*, 660(1):823–844, May 2007. doi: 10.1086/512759.

M. Marks, E. L. Martín, V. J. S. Béjar, et al. Using binary statistics in Taurus-Auriga to distinguish between brown dwarf formation processes. *A&A*, 605: A11, August 2017. doi: 10.1051/0004-6361/201629457.

C. B. Markwardt. Non-linear Least-squares Fitting in IDL with MPFIT. In D. A. Bohlender, D. Durand, and P. Dowler, editors, *Astronomical Data Analysis Software and Systems XVIII*, volume 411 of *Astronomical Society of the Pacific Conference Series*, page 251, September 2009.

F. Masset and M. Snellgrove. Reversing type II migration: resonance trapping of a lighter giant protoplanet. *MNRAS*, 320(4):L55–L59, February 2001. doi: 10.1046/j.1365-8711.2001.04159.x.

Sean P. Matt, A. Sacha Brun, Isabelle Baraffe, et al. The Mass-dependence of Angular Momentum Evolution in Sun-like Stars. *ApJ*, 799(2):L23, January 2015. doi: 10.1088/2041-8205/799/2/L23.

Michel Mayor and Didier Queloz. A Jupiter-mass companion to a solar-type star. *Nature*, 378(6555):355–359, November 1995. doi: 10.1038/378355a0.

R. G. McMahon, M. Banerji, E. Gonzalez, et al. First Scientific Results from the VISTA Hemisphere Survey (VHS). *The Messenger*, 154:35–37, December 2013.

Søren Meibom, Robert D. Mathieu, and Keivan G. Stassun. Stellar Rotation in M35: Mass-Period Relations, Spin-Down Rates, and Gyrochronology. *ApJ*, 695(1):679–694, April 2009. doi: 10.1088/0004-637X/695/1/679.

Søren Meibom, Sydney A. Barnes, David W. Latham, et al. The Kepler Cluster Study: Stellar Rotation in NGC 6811. *ApJ*, 733(1):L9, May 2011. doi: 10.1088/2041-8205/733/1/L9.

Erin Mentuch, Alexis Brandeker, Marten H. van Kerkwijk, et al. Lithium Depletion of Nearby Young Stellar Associations. *ApJ*, 689(2):1127–1140, December 2008. doi: 10.1086/592764.

Stanimir A. Metchev, J. Davy Kirkpatrick, G. Bruce Berriman, et al. A Cross-Match of 2MASS and SDSS: Newly Found L and T Dwarfs and an Estimate of the Space Density of T Dwarfs. *ApJ*, 676(2):1281–1306, April 2008. doi: 10.1086/524721.

H. Mizuno. Formation of the Giant Planets. *Progress of Theoretical Physics*, 64 (2):544–557, August 1980. doi: 10.1143/PTP.64.544.

J. Montalbán and R. Rebolo. Planet accretion and the abundances of lithium isotopes. *A&A*, 386:1039–1043, May 2002. doi: 10.1051/0004-6361:20020338.

A. Morbidelli, B. Bitsch, A. Crida, et al. Fossilized condensation lines in the Solar System protoplanetary disk. *Icarus*, 267:368–376, March 2016. doi: 10.1016/j.icarus.2015.11.027.

Kazumasa Moriwaki and Yoshitsugu Nakagawa. A Planetesimal Accretion Zone in a Circumbinary Disk. *ApJ*, 609(2):1065–1070, July 2004. doi: 10.1086/421342.

N. Murray, B. Hansen, M. Holman, et al. Migrating Planets. *Science*, 279:69, January 1998. doi: 10.1126/science.279.5347.69.

Koraljka Mužić, Alexander Scholz, Vincent C. Geers, et al. Substellar Objects in Nearby Young Clusters (SONYC) IX: The Planetary-Mass Domain of Chamaeleon-I and Updated Mass Function in Lupus-3. *ApJ*, 810(2):159, September 2015. doi: 10.1088/0004-637X/810/2/159.

Koraljka Mužić, Rainer Schödel, Alexander Scholz, et al. The low-mass content of the massive young star cluster RCW 38. *MNRAS*, 471(3):3699–3712, November 2017. doi: 10.1093/mnras/stx1906.

T. Nakajima, B. R. Oppenheimer, S. R. Kulkarni, et al. Discovery of a cool brown dwarf. *Nature*, 378(6556):463–465, November 1995. doi: 10.1038/378463a0.

Richard P. Nelson. On the evolution of giant protoplanets forming in circumbinary discs. *MNRAS*, 345(1):233–242, October 2003. doi: 10.1046/j.1365-8711.2003.06929.x.

Eric L. Nielsen, Robert J. De Rosa, Bruce Macintosh, et al. The Gemini Planet Imager Exoplanet Survey: Giant Planet and Brown Dwarf Demographics from 10 to 100 au. *AJ*, 158(1):13, July 2019. doi: 10.3847/1538-3881/ab16e9.

R. W. Noyes, L. W. Hartmann, S. L. Baliunas, et al. Rotation, convection, and magnetic activity in lower main-sequence stars. *ApJ*, 279:763–777, April 1984. doi: 10.1086/161945.

Karin I. Öberg, Ruth Murray-Clay, and Edwin A. Bergin. The Effects of Snowlines on C/O in Planetary Atmospheres. *ApJ*, 743(1):L16, December 2011. doi: 10.1088/2041-8205/743/1/L16.

Paolo Padoan and Åke Nordlund. The Stellar Initial Mass Function from Turbulent Fragmentation. *ApJ*, 576(2):870–879, September 2002. doi: 10.1086/341790.

Paolo Padoan and Åke Nordlund. The "Mysterious" Origin of Brown Dwarfs. *ApJ*, 617(1):559–564, December 2004. doi: 10.1086/345413.

R. Pallavicini, L. Golub, R. Rosner, et al. Relations among stellar X-ray emission observed from Einstein, stellar rotation and bolometric luminosity. *ApJ*, 248:279–290, August 1981. doi: 10.1086/159152.

E. Palle, R. Luque, M. R. Zapatero Osorio, et al. ESPRESSO mass determination of TOI-263b: an extreme inhabitant of the brown dwarf desert. *A&A*, 650:A55, June 2021. doi: 10.1051/0004-6361/202039937.

Xiaoying Pang, Yuqian Li, Zeqiu Yu, et al. 3D Morphology of Open Clusters in the Solar Neighborhood with Gaia EDR 3: Its Relation to Cluster Dynamics. *ApJ*, 912(2):162, May 2021. doi: 10.3847/1538-4357/abeaac.

Ruskin Patel and Kaloyan Penev. Constraining tidal quality factor using spin period in eclipsing binaries. *MNRAS*, 512(3):3651–3661, May 2022. doi: 10.1093/mnras/stac203.

Shannon G. Patel, Steven S. Vogt, Geoffrey W. Marcy, et al. Fourteen New Companions from the Keck and Lick Radial Velocity Survey Including Five Brown Dwarf Candidates. *ApJ*, 665(1):744–753, August 2007. doi: 10.1086/519066.

E. Paunzen. A new catalogue of Strömgren-Crawford uvbyβ photometry. *A&A*, 580:A23, August 2015. doi: 10.1051/0004-6361/201526413.

Kaloyan Penev, Brian Jackson, Federico Spada, et al. Constraining Tidal Dissipation in Stars from the Destruction Rates of Exoplanets. *ApJ*, 751(2):96, Jun 2012. doi: 10.1088/0004-637X/751/2/96.

Kaloyan Penev, L. G. Bouma, Joshua N. Winn, et al. Empirical Tidal Dissipation in Exoplanet Hosts From Tidal Spin-up. *AJ*, 155(4):165, April 2018. doi: 10.3847/1538-3881/aaaf71.

F. Perri and A. G. W. Cameron. Hydrodynamic Instability of the Solar Nebula in the Presence of a Planetary Core. *Icarus*, 22(4):416–425, August 1974. doi: 10.1016/0019-1035(74)90074-8.

Carina M. Persson, Szilárd Csizmadia, Alexander J. Mustill, et al. Greening of the brown-dwarf desert. EPIC 212036875b: a 51 M_J object in a 5-day orbit around an F7 V star. *A&A*, 628:A64, August 2019. doi: 10.1051/0004-6361/201935505.

D. J. Pinfield, B. Burningham, M. Tamura, et al. Fifteen new T dwarfs discovered in the UKIDSS Large Area Survey. *MNRAS*, 390(1):304–322, October 2008. doi: 10.1111/j.1365-2966.2008.13729.x.

M. Pinsonneault. Mixing in Stars. *ARA&A*, 35:557–605, January 1997. doi: 10.1146/annurev.astro.35.1.557.

M. H. Pinsonneault, Steven D. Kawaler, S. Sofia, et al. Evolutionary Models of the Rotating Sun. *ApJ*, 338:424, March 1989. doi: 10.1086/167210.

Nikolai Piskunov and Jeff A. Valenti. Spectroscopy Made Easy: Evolution. *A&A*, 597:A16, January 2017. doi: 10.1051/0004-6361/201629124.

Ana-Maria A. Piso, Karin I. Öberg, Tilman Birnstiel, et al. C/O and Snowline Locations in Protoplanetary Disks: The Effect of Radial Drift and Viscous Gas Accretion. *ApJ*, 815(2):109, December 2015. doi: 10.1088/0004-637X/815/2/109.

N. Pizzolato, A. Maggio, G. Micela, et al. The stellar activity-rotation relationship revisited: Dependence of saturated and non-saturated X-ray emission regimes on stellar mass for late-type dwarfs. *A&A*, 397:147–157, January 2003. doi: 10.1051/0004-6361:20021560.

B. Plez. Turbospectrum: Code for spectral synthesis. Astrophysics Source Code Library, record ascl:1205.004, May 2012.

James B. Pollack, Olenka Hubickyj, Peter Bodenheimer, et al. Formation of the Giant Planets by Concurrent Accretion of Solids and Gas. *Icarus*, 124(1):62–85, November 1996. doi: 10.1006/icar.1996.0190.

S. Randich, J. H. M. M. Schmitt, C. F. Prosser, et al. The X-ray properties of the young open cluster around α Persei. *A&A*, 305:785, January 1996.

Frederic A. Rasio and Eric B. Ford. Dynamical instabilities and the formation of extrasolar planetary systems. *Science*, 274:954–956, November 1996. doi: 10.1126/science.274.5289.954.

H. Rauer, C. Catala, C. Aerts, et al. The PLATO 2.0 mission. *Experimental Astronomy*, 38(1-2):249–330, November 2014. doi: 10.1007/s10686-014-9383-4.

Sean N. Raymond, Avi M. Mandell, and Steinn Sigurdsson. Exotic Earths: Forming Habitable Worlds with Giant Planet Migration. *Science*, 313(5792):1413–1416, September 2006. doi: 10.1126/science.1130461.

Sean N. Raymond, Philip J. Armitage, and Noel Gorelick. Planet-Planet Scattering in Planetesimal Disks. *ApJ*, 699(2):L88–L92, July 2009. doi: 10.1088/0004-637X/699/2/L88.

Sean N. Raymond, Philip J. Armitage, and Noel Gorelick. Planet-Planet Scattering in Planetesimal Disks. II. Predictions for Outer Extrasolar Planetary Systems. *ApJ*, 711(2):772–795, March 2010. doi: 10.1088/0004-637X/711/2/772.

R. Rebolo, M. R. Zapatero Osorio, and E. L. Martín. Discovery of a brown dwarf in the Pleiades star cluster. *Nature*, 377(6545):129–131, September 1995. doi: 10.1038/377129a0.

L. M. Rebull, S. C. Wolff, and S. E. Strom. Stellar Rotation in Young Clusters: The First 4 Million Years. *AJ*, 127(2):1029–1051, February 2004. doi: 10.1086/380931.

L. M. Rebull, J. R. Stauffer, J. Bouvier, et al. Rotation in the Pleiades with K2. II. Multiperiod Stars. *AJ*, 152(5):114, November 2016. doi: 10.3847/0004-6256/152/5/114.

L. M. Rebull, J. R. Stauffer, A. M. Cody, et al. Rotation of Low-mass Stars in Taurus with K2. *AJ*, 159(6):273, June 2020. doi: 10.3847/1538-3881/ab893c.

George R. Ricker, Joshua N. Winn, Roland Vanderspek, et al. Transiting Exoplanet Survey Satellite (TESS). *Journal of Astronomical Telescopes, Instruments, and Systems*, 1:014003, January 2015. doi: 10.1117/1.JATIS.1.1.014003.

Adric R. Riedel, Sarah C. Blunt, Erini L. Lambrides, et al. LACEwING: A New Moving Group Analysis Code. *AJ*, 153(3):95, March 2017. doi: 10.3847/1538-3881/153/3/95.

J. Sahlmann, D. Ségransan, D. Queloz, et al. Search for brown-dwarf companions of stars. *A&A*, 525:A95, January 2011. doi: 10.1051/0004-6361/201015427.

Eric L. Sandquist, Jon J. Dokter, D. N. C. Lin, et al. A Critical Examination of Li Pollution and Giant-Planet Consumption by a Host Star. *ApJ*, 572(2):1012–1023, June 2002. doi: 10.1086/340452.

N. C. Santos, G. Israelian, M. Mayor, et al. Statistical properties of exoplanets. II. Metallicity, orbital parameters, and space velocities. *A&A*, 398:363–376, January 2003. doi: 10.1051/0004-6361:20021637.

E. Schatzman. A theory of the role of magnetic activity during star formation. *Annales d'Astrophysique*, 25:18, February 1962.

J. Schneider, C. Dedieu, P. Le Sidaner, et al. Defining and cataloging exoplanets: the exoplanet.eu database. *A&A*, 532:A79, August 2011. doi: 10.1051/0004-6361/201116713.

Alexander Scholz, Ray Jayawardhana, Koraljka Muzic, et al. Substellar Objects in Nearby Young Clusters (SONYC). VI. The Planetary-mass Domain of NGC 1333. *ApJ*, 756(1):24, September 2012. doi: 10.1088/0004-637X/756/1/24.

Alexander Scholz, Vincent Geers, Paul Clark, et al. Substellar Objects in Nearby Young Clusters. VII. The Substellar Mass Function Revisited. *ApJ*, 775(2): 138, October 2013. doi: 10.1088/0004-637X/775/2/138.

Aldo Serenelli, Achim Weiss, Conny Aerts, et al. Weighing stars from birth to death: mass determination methods across the HRD. *A&A Rev.*, 29(1):4, December 2021. doi: 10.1007/s00159-021-00132-9.

L. Siess, E. Dufour, and M. Forestini. An internet server for pre-main sequence tracks of low- and intermediate-mass stars. *A&A*, 358:593–599, June 2000.

Robert J. Siverd, Karen A. Collins, George Zhou, et al. KELT-19Ab: A P $\sim$ 4.6-day Hot Jupiter Transiting a Likely Am Star with a Distant Stellar Companion. *AJ*, 155(1):35, January 2018. doi: 10.3847/1538-3881/aa9e4d.

M. F. Skrutskie, R. M. Cutri, R. Stiening, et al. The Two Micron All Sky Survey (2MASS). *AJ*, 131(2):1163–1183, February 2006. doi: 10.1086/498708.

A. Skumanich. Time Scales for Ca II Emission Decay, Rotational Braking, and Lithium Depletion. *ApJ*, 171:565, February 1972. doi: 10.1086/151310.

Catherine L. Slesnick, Lynne A. Hillenbrand, and John M. Carpenter. The Spectroscopically Determined Substellar Mass Function of the Orion Nebula Cluster. *ApJ*, 610(2):1045–1063, August 2004. doi: 10.1086/421898.

B. Smalley, J. Southworth, O. I. Pintado, et al. Eclipsing Am binary systems in the SuperWASP survey. *A&A*, 564:A69, April 2014. doi: 10.1051/0004-6361/201323158.

Chris Sneden, Jacob Bean, Inese Ivans, et al. MOOG: LTE line analysis and spectrum synthesis. Astrophysics Source Code Library, record ascl:1202.009, February 2012.

D. R. Soderblom, M. S. Oey, D. R. H. Johnson, et al. The Evolution of the Lithium Abundances of Solar-Type Stars. I. The Hyades and Coma Berenices Clusters. *AJ*, 99:595, February 1990. doi: 10.1086/115353.

David R. Soderblom. The Ages of Stars. *ARA&A*, 48:581–629, September 2010. doi: 10.1146/annurev-astro-081309-130806.

David R. Soderblom, Stephen B. Fedele, Burton F. Jones, et al. The Evolution of the Lithium Abundances of Solar-Type Stars. IV. Praesepe. *AJ*, 106:1080, September 1993a. doi: 10.1086/116705.

David R. Soderblom, Burton F. Jones, Suchitra Balachandran, et al. The Evolution of the Lithium Abundances of Solar-Type Stars. III. The Pleiades. *AJ*, 106:1059, September 1993b. doi: 10.1086/116704.

David R. Soderblom, Catherine A. Pilachowski, Stephen B. Fedele, et al. The Evolution of the Lithium Abundances of Solar-Type Stars. II. the Ursa Major Group. *AJ*, 105:2299, June 1993c. doi: 10.1086/116608.

David R. Soderblom, Burton F. Jones, John R. Stauffer, et al. The Evolution of the Lithium Abundances of Solar-Type Stars.V. K Dwarfs in the Hyades. *AJ*, 110:729, August 1995. doi: 10.1086/117556.

D. S. Spiegel, A. Burrows, and J. A. Milsom. The Deuterium-burning Mass Limit for Brown Dwarfs and Giant Planets. *ApJ*, 727:57, January 2011. doi: 10.1088/0004-637X/727/1/57.

A. Suárez Mascareño, M. Damasso, N. Lodieu, et al. Rapid contraction of giant planets orbiting the 20-million-year-old star V1298 Tau. *Nature Astronomy*, December 2021. doi: 10.1038/s41550-021-01533-7.

Y. Takeda, S. Honda, S. Kawanomoto, et al. Behavior of Li abundances in solar-analog stars. II. Evidence of the connection with rotation and stellar activity. *A&A*, 515:A93, June 2010. doi: 10.1051/0004-6361/200913897.

Ingo Thies and Pavel Kroupa. A Discontinuity in the Low-Mass Initial Mass Function. *ApJ*, 671(1):767–780, December 2007. doi: 10.1086/522512.

Ingo Thies and Pavel Kroupa. A discontinuity in the low-mass IMF - the case of high multiplicity. *MNRAS*, 390(3):1200–1206, November 2008. doi: 10.1111/j.1365-2966.2008.13827.x.

Ingo Thies, Pavel Kroupa, Simon P. Goodwin, et al. Tidally Induced Brown Dwarf and Planet Formation in Circumstellar Disks. *ApJ*, 717(1):577–585, July 2010. doi: 10.1088/0004-637X/717/1/577.

Ingo Thies, Jan Pflamm-Altenburg, Pavel Kroupa, et al. Characterizing the Brown Dwarf Formation Channels from the Initial Mass Function and Binary-star Dynamics. *ApJ*, 800(1):72, February 2015. doi: 10.1088/0004-637X/800/1/72.

G. Torres, J. Andersen, and A. Giménez. Accurate masses and radii of normal stars: modern results and applications. *A&A Rev.*, 18(1-2):67–126, February 2010. doi: 10.1007/s00159-009-0025-1.

C. A. Tout and J. E. Pringle. Spin-down of rapidly rotating, convective stars. *MNRAS*, 256:269–276, May 1992. doi: 10.1093/mnras/256.2.269.

D. E. Trilling, W. Benz, T. Guillot, et al. Orbital Evolution and Migration of Giant Planets: Modeling Extrasolar Planets. *ApJ*, 500(1):428–439, June 1998. doi: 10.1086/305711.

J. A. Valenti and N. Piskunov. Spectroscopy made easy: A new tool for fitting observations with synthetic spectra. *A&AS*, 118:595–603, September 1996.

Jennifer L. van Saders and Marc H. Pinsonneault. Fast Star, Slow Star; Old Star, Young Star: Subgiant Rotation as a Population and Stellar Physics Diagnostic. *ApJ*, 776(2):67, October 2013. doi: 10.1088/0004-637X/776/2/67.

Jennifer L. van Saders, Tugdual Ceillier, Travis S. Metcalfe, et al. Weakened magnetic braking as the origin of anomalously rapid rotation in old field stars. *Nature*, 529(7585):181–184, January 2016. doi: 10.1038/nature16168.

Paolo Ventura, Anna Zeppieri, Italo Mazzitelli, et al. Pre-main sequence Lithium burning: the quest for a new structural parameter. *A&A*, 331:1011–1021, March 1998.

W. Voges, B. Aschenbach, Th. Boller, et al. The ROSAT all-sky survey bright source catalogue. *A&A*, 349:389–405, September 1999.

Steven S. Vogt, R. Paul Butler, Geoffrey W. Marcy, et al. Ten Low-Mass Companions from the Keck Precision Velocity Survey. *ApJ*, 568(1):352–362, March 2002. doi: 10.1086/338768.

Kaspar von Braun, Tabetha S. Boyajian, Gerard T. van Belle, et al. Stellar diameters and temperatures - V. 11 newly characterized exoplanet host stars. *MNRAS*, 438(3):2413–2425, March 2014. doi: 10.1093/mnras/stt2360.

E. I. Vorobyov. Ejection of gaseous clumps from gravitationally unstable protostellar disks. *A&A*, 590:A115, May 2016. doi: 10.1051/0004-6361/201628102.

J. Šubjak, M. Endl, P. Chaturvedi, et al. TOI-1268b: The youngest hot Saturn-mass transiting exoplanet. *A&A*, 662:A107, June 2022. doi: 10.1051/0004-6361/202142883.

Ján Šubjak, Rishikesh Sharma, Theron W. Carmichael, et al. TOI-503: The First Known Brown-dwarf Am-star Binary from the TESS Mission. *AJ*, 159(4):151, April 2020. doi: 10.3847/1538-3881/ab7245.

Anthony P. Whitworth. *Brown Dwarf Formation: Theory*, page 95. 2018. doi: 10.1007/978-3-319-55333-7_95.

Edward L. Wright, Peter R. M. Eisenhardt, Amy K. Mainzer, et al. The Wide-field Infrared Survey Explorer (WISE): Mission Description and Initial On-orbit Performance. *AJ*, 140(6):1868–1881, December 2010. doi: 10.1088/0004-6256/140/6/1868.

J. T. Wright, O. Fakhouri, G. W. Marcy, et al. The Exoplanet Orbit Database. *PASP*, 123(902):412, April 2011. doi: 10.1086/659427.

Samuel W. Yee, Erik A. Petigura, and Kaspar von Braun. Precision Stellar Characterization of FGKM Stars using an Empirical Spectral Library. *ApJ*, 836(1):77, February 2017. doi: 10.3847/1538-4357/836/1/77.

Donald G. York, J. Adelman, Jr. Anderson, John E., et al. The Sloan Digital Sky Survey: Technical Summary. *AJ*, 120(3):1579–1587, September 2000. doi: 10.1086/301513.

G. Zhou, G. Á. Bakos, D. Bayliss, et al. HATS-70b: A 13 MJ brown dwarf transiting an a star. *The Astronomical Journal*, 157(1):31, jan 2019. doi: 10.3847/1538-3881/aaf1bb.

List of Figures

1.1 Comparison between the theoretical IMF (solid line), and stellar/brown dwarf system IMF representative of the Galactic field and young clusters (dotted line) (Chabrier, 2003). The bottom axis is in units of solar masses. We can see that the theoretical model does not reproduce the observed abundance of brown dwarfs with M$\leq$ 0.08 $M_{\odot}$. Source: Hennebelle and Chabrier (2008). . . . 7

1.2 Mass-ratio vs primary mass distribution. Upper panel: Binaries formed by random pairing over the complete mass range of a single population of BDs and stars (grey points) and the observations of the Chamaeleon I star-forming region (black diamonds) (Lafrenière et al., 2008). Lower panel: Binaries formed by random pairing of stars with $M_{\star}$ above 0.075. If the binaries were formed by random pairing over the complete mass range of a single population of BDs and stars, we would observe lower mass ratios. The observations agree well with a random pairing of stars as the separate population. Source: Thies and Kroupa (2008) 9

1.3 Percentage of the currently known transiting BDs vs spectral type of host star. 10

1.4 Planetary minimum mass versus orbital period for the known planets characterised by radial velocity. In the top panel, we can see the kernel density estimate of planetary orbital periods for the mass range of Jovian planets between 0.1 and 15 M_J revealing the bimodal distribution. Data from Fontanive and Bardalez Gagliuffi (2021). 12

1.5 Planet fraction ($N_{planets}/N_{stars}$) as a function of stellar metallicity for the sample of 1266 stars drawn from the California Planet Survey (gray histogram) (Johnson et al., 2010). The filled red circles represent the median planet fraction of the stars in each bin. The blue diamonds represent the planet fraction for solar-like stars. Source: Johnson et al. (2010). 13

1.6 Luminosity vs effective temperature plot. Curves represent MIST isochrones for ages: 30 Myr (blue), 50 Myr (orange), 100 Myr (green), 1 Gyr (red), 6 Gyr (purple), 10 Gyr (brown). 18

1.7 Color-period diagram of members of well-studied clusters: Pleiades cluster, M34 cluster, M37 cluster, M48 cluster, Praesepe cluster, NGC 6811 cluster, and NGC 6774 cluster. Lines represent the 100, 400, 650, and 2500 Myr curves computed from the empirical relation from Angus et al. (2019b). 20

1.8 Colour vs EW of lithium line Li 6708 Å for members of well-studied clusters: Tuc-Hor young moving group, the Pleiades, M34, Ursa Major Group, Praesepe, Hyades, and M67 clusters. 22

1.9 X-ray luminosity vs colour for members of well-defined clusters from Jackson et al. (2012). 24

1.10 $B-V$ colour vs logR'$_{HK}$ for members of several well-studied stellar clusters from (Mamajek and Hillenbrand, 2008): Sco-Cen members, Pleiades, Hyades, and M67. Source: Mamajek and Hillenbrand (2008). 25
1.11 Membership to young associations. Ellipses represent the 1-sigma position of young stellar associations in space velocities U, V, W taken from Gagné et al. (2018). 25

2.1 Eccentricity versus orbital period for the known planets characterised by radial velocity. Data from Fontanive and Bardalez Gagliuffi (2021). 26

List of Abbreviations

SSO	Substellar object
BD	Brown dwarf
EGP	Extrasolar giant planet
M_J	Mass of Jupiter
R_J	Radius of Jupiter
$M_\odot$	Solar mass
$R_\odot$	Solar radius
SED	Spectral energy distribtion
EW_{Li}	Lithium equivalent width
IMF	Initial mass function
H-R diagram	Hertzsprung–Russell diagram
MS	Main sequence
Myr	Million years
Gyr	Billion years
EW	Equivalent width
au	Astronomical unit
2MASS	Two-Micron All-Sky Survey
WISE	Wide-field Infrared Survey Explorer
DENIS	Deep Near-Infrared Survey of the Southern Sky
UKIDSS	UKIRT Infrared Deep Sky Survey
VHS	VISTA Hemisphere Survey
DES	Dark Energy Survey
SDSS	Sloan Digital Sky Survey
Pan-STARRS	Panoramic Survey Telescope and Rapid Response System

List of publications

(1) Ján Šubjak, Rishikesh Sharma, Theron W. Carmichael, et al. TOI-503: The First Known Brown-dwarf Am-star Binary from the TESS Mission. *AJ*, 159(4):151, April 2020.
(2) J. Šubjak, M. Endl, P. Chaturvedi, et al. TOI-1268b: The youngest hot Saturn-mass transiting exoplanet. *A&A*, 662:A107, June 2022.
(3) Pavol Gajdoš, Martin Vaňko, Theodor Pribulla, et al. Transit timing variations, radial velocities, and long-term dynamical stability of the system Kepler-410. *MNRAS*, 484(3):4352–4359, April 2019.
(4) Carina M. Persson, Szilárd Csizmadia, Alexander J. Mustill, et al. Greening of the brown-dwarf desert. EPIC 212036875b: a 51 M_J object in a 5-day orbit around an F7 V star. *A&A*, 628:A64, August 2019.
(5) P. Kabáth, M. Skarka, S. Sabotta, et al. Ondřejov Echelle Spectrograph, Ground Based Support Facility for Exoplanet Missions. *PASP*, 132:035002, March 2020.
(6) Kristine W. F. Lam, Judith Korth, Kento Masuda, et al. It Takes Two Planets in Resonance to Tango around K2-146. *AJ*, 159(3):120, March 2020.
(7) D. Hidalgo, E. Pallé, R. Alonso, et al. Three planets transiting the evolved star EPIC 249893012: a hot 8.8-$M_\oplus$ super-Earth and two warm 14.7 and 10.2-$M_\oplus$ sub-Neptunes. *A&A*, 636:A89, April 2020.
(8) P. Bluhm, R. Luque, N. Espinoza, et al. Precise mass and radius of a transiting super-Earth planet orbiting the M dwarf TOI-1235: a planet in the radius gap? *A&A*, 639:A132, July 2020.
(9) Grzegorz Nowak, Enric Palle, Davide Gandolfi, et al. K2-280 b - a low density warm sub-Saturn around a mildly evolved star. *MNRAS*, 497(4):4423–4435, October 2020.
(10) M. Fridlund, J. Livingston, D. Gandolfi, et al. The TOI-763 system: sub-Neptunes orbiting a Sun-like star. *MNRAS*, 498(3):4503–4517, November 2020.
(11) R. Luque, L. M. Serrano, K. Molaverdikhani, et al. A planetary system with two transiting mini-Neptunes near the radius valley transition around the bright M dwarf TOI-776. *A&A*, 645:A41, January 2021.
(12) S. Hoyer, D. Gandolfi, D. J. Armstrong, et al. TOI-220 b: a warm sub-Neptune discovered by TESS. *MNRAS*, 505(3):3361–3379, August 2021.
(13) V. Van Eylen, N. Astudillo-Defru, X. Bonfils, et al. Masses and compositions of three small planets orbiting the nearby M dwarf L231-32 (TOI-270) and the M dwarf radius valley. *MNRAS*, 507(2):2154–2173, October 2021.
(14) Kristine W. F. Lam, Szilárd Csizmadia, Nicola Astudillo-Defru, et al. GJ 367b: A dense, ultrashort-period sub-Earth planet transiting a nearby red dwarf star., *Science*, 374(6572):1271–1275, December 2021.
(15) Quang H. Tran, Brendan P. Bowler, Michael Endl, et al. TOI-1670 b and c: An Inner Sub-Neptune with an Outer Warm Jupiter Unlikely to Have Originated from High-eccentricity Migration. *AJ*, 163(5):225, May 2022.
(16) Martin Blažek, Petr Kabáth, Anjali A. A. Piette, et al. Constraints on TESS albedos for five hot Jupiters. *MNRAS*, 513(3):3444–3457, July 2022.
(17) Petr Kabáth, Priyanka Chaturvedi, Phillip J. MacQueen, et al. TOI-2046b, TOI-1181b, and TOI-1516b, three new hot Jupiters from TESS: planets orbiting

a young star, a subgiant, and a normal star. *MNRAS*, 513(4):5955–5972, July 2022.
(18) O. Barragán, D. J. Armstrong, D. Gandolfi, et al. The young HD 73583 (TOI-560) planetary system: two 10-$M_\oplus$ mini-Neptunes transiting a 500-Myr-old, bright, and active K dwarf. *MNRAS*, 514(2):1606–1627, August 2022.
(19) J. Šubjak, N. Lodieu, P. Kabáth, et al. Search for planets around stars with wide brown dwarfs. Accepted for publication in *A&A*.
(20) J. Korth, D. Gandolfi, J. Šubjak, et al. TOI-1130: A photodynamical analysis of a hot Jupiter in resonance with an inner low-mass planet. Submitted for publication to *A&A*.